V. CONCLUSIONS

The results presented in this report, and those of previous studies (Dwyer and Turner, 1982; Summers, 1985; Dwyer, 1985) have 1) defined the major factors controlling DO distributions in the lower Conowingo Reservoir and the downstream river reach, and 2) indicated the efficacy of various continuous minimum discharges for improving discharge DO. All of these studies have led to the following conclusions about factors controlling the discharge DO from Conowingo Reservoir:

- The decomposition of organic matter in the water column of the reservoir results in oxygen depletion in the reservoir; as a consequence, the severity of DO depletion in the summertime increases due mostly to longer water residence time caused by low summer river flow (Summers, 1985). Longer residence times and higher temperatures produce a complex set of biological interactions that result ultimately in severe oxygen depletion (Dwyer, 1985).

- Water residence time in the reservoir is controlled by river flow; water flushing at a rate fast enough to overcome the DO depletion occurs only at average daily river flows greater than approximately 20,000 cfs (Gannett Fleming Environmental Engineers, Inc. 1985). The general relationship between historical DO concentrations and river flows over the period 1970 to 1980 is shown in Fig. V-1.

- Any continuous minimum discharge schedule acts only to reallocate the available water (determined by average river flow) within a day or at most a week. If these reallocations result in a daily average turbine discharge above 20,000 cfs for a short period, then discharge DO values will be increased temporarily. For example, in Figure IV-3 the weekday peaking scenario concentrates all the available river flow (16,050 cfs) into 5 days; thus, an average discharge on each weekday is 7/5 • 16,000 or 22,400 cfs, and discharge DO increases until the following weekend shutdown.

  In general, no generating schedule incorporating a continuous minimum discharge (including run-of-river) at average or low river flows will provide enough sustained improvement in discharge DO to allow it to meet the state water quality standard for DO. The only way in which a minimum flow might increase discharge DO values is if low DO water in the reservoir is flushed

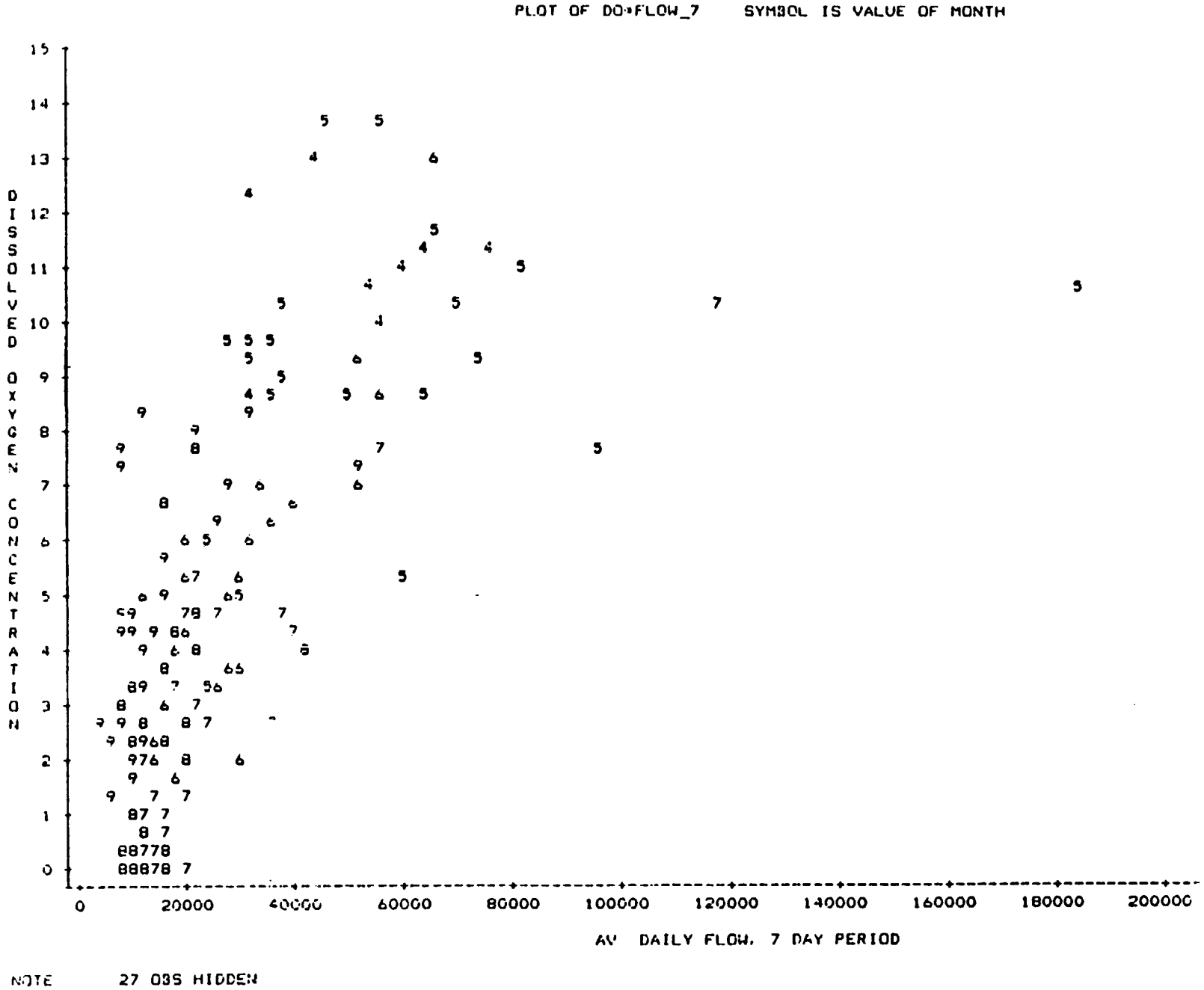

Figure V-1. DO concentration (mg/l) in bottom layer of reservoir (1970-1980) vs. weekly average of daily flow from Conowingo Dam. Symbol is month of the year. Data from PECO monitoring studies of the Peach Bottom Atomic Power Station on Conowingo Reservoir (unpublished).

out, or oxygenated surface reservoir water is preferentially withdrawn. Neither of these possibilities in fact occurs:

-- Minimum discharges do not increase water exchange or flushing enough to increase average reservoir DO concentrations.

-- Simulations of the withdrawal of more surface water (as simulated by the WES model) indicated that only negligible increases in the discharge DO would result (see Fig. III-2).

-- The model results indicate that withdrawal exclusively from the surface layer would result in the greatest improvement in DO. However, this would entail the construction of a withdrawal tower or other surface intake structure for the turbines. Also, since surface DO values are frequently less than 5 ppm, surface withdrawal could not assure that the discharge DO could comply with the state standard at all times.

- The DO concentration of the discharge can increase only if:

  -- Oxygen is added to waters in the reservoir or during discharge from the reservoir (e.g., in the turbines) or

  -- Organic matter is removed or otherwise controlled in the reservoir or at its sources.

  The suspended particulate matter and nutrient loads of the Susquehanna River have been identified as the major contributor to DO depletion in the Chesapeake Bay (Chesapeake Bay Program, 1982). Non-point source control of sediment and nutrient inputs from the 27,000 square miles of the Susquehanna River watershed was recommended as a management priority. However, even if non-point source controls are imposed in the watershed, their effects on DO depletion in Conowingo Reservoir cannot be forecast easily because of:

  -- The length of time needed to implement the control strategy and determine its ultimate effectiveness

  -- The probability that the large quantity of organic matter stored in bottom sediments will be resuspended during wind-driven or other high-energy mixing events, and cause DO depletion.

The alternative is to artificially add enough oxygen to the water to meet the Maryland standard. This approach is being implemented at the Safe Harbor project in order to comply with Pennsylvania water quality standards The feasibility of implementing a similar approach at Conowingo is presently being assessed.

VI. REFERENCES

Bohan, J.P. and J.L. Grace, Jr. 1973. Selective withdrawal from man-made lakes; hydraulic laboratory investigation. U.S. Army Engineer Waterways Experiment Station, Vicksburg, MS. Technical Report H-73-4.

Chesapeake Bay Program. 1982. Chesapeake Bay Program Technical Studies: a synthesis. U.S. Environmental Protection Agency, Washington, DC.

Davis, J.C. 1975. Minimal dissolved oxygen requirements of aquatic life with emphasis on Canadian species: a review. J. Fish. Res. Board Can. 32:2295-2332.

Debler, W.R. 1959. Stratified flow into a line sink, ASCE Journal of Engineering Mechanics Division, Vol. 85, EM3.

Dwyer, R.L. and M.A. Turner. 1982. Simulation of river flow and DO dynamics affected by peaking discharges from a hydroelectric dam. Maryland Power Plant Siting Program. Report PPSP-UBLS-82-3. Annapolis, MD.

Gannett Fleming Environmental Engineers, Inc. 1985. Preliminary evaluation of aeration alternatives for Conowingo Dam. Prepared for Maryland Power Plant Siting Program. Technical Memorandum T-85-4 (unpublished).

Kremer, J.M. and S.W. Nixon. 1978. A Coastal Marine Ecosystem: Simulation and Analysis. Berlin: Springer-Verlag.

Krenkel, P.A. and V. Novotny. 1980. Water Quality Management. New York: Academic Press.

Mejer, H. 1983. The computer as a modeling tool. pp. 17-53 in Jorgensen, S.E. Application of ecological modeling in environmental management, Part A. Elsevier, Amsterdam.

Parsons, T.R. and M. Takahashi. 1973. Biological Oceanographic Processes. New York: Pergamon Press.

Philipp, K.R. and P.N. Klose. 1981. Lower Susquehanna River oxygen dynamics study. Maryland Power Plant Siting Program Report No. PPSP-UBLS-81-4. Annapolis, Md.

Potera, G.T., K.R. Phillip, T.D. Johnson, H.J. Petrimoulx, and P.N. Klose. 1982. Lower Susquehanna River hydrographic and water quality study, summer 1981. Maryland Power Plant Siting Program, Report PPSP-UBLS-82-2. Annapolis, MD.

Sanders, J.G., K.R. Kaumeyer, and W.R. Boynton. 1982a. Plankton metabolism and benthic respiration in the Conowingo Reservoir. Prepared for Radiation Management Corp. February 1982.

Kaumeyer, K.R. 1982b. Plankton metabolism, benthic metabolism, and oxygen diffusion in the Conowingo Reservoir. Prepared for Radiation Management Corp. October 1982.

Summers, J.K. 1985. The Conowingo Reservoir ecosystem simulation model. Maryland Power Plant Siting Program Report No. PPSP-UBLS-85-2. Annapolis, MD.

Wetzel, R.G. 1975. Limnology. Philadelphia: W.B. Saunders.

Yih, Chia-Shun. 1965. Dynamics of Nonhomogeneous Fluids. New York: The MacMillan Company.

APPENDIX A

EMPIRICAL ESTIMATION OF WATER WITHDRAWAL FROM CONOWINGO RESERVOIR

Prepared By:

Martha A. Turner
Robert L. Dwyer

A.I. INTRODUCTION

Maryland Department of Natural Resources (DNR) is one of several organizations which have intervened in the Federal Energy Regulatory Commission's (FERC) relicensing of the Conowingo Hydroelectric Facility on the Susquehanna River. The Power Plant Siting Program (PPSP) was designated by DNR as the lead agency for relicensing activities; as PPSP's Aquatic Integrator, Martin Marietta Environmental Systems is responsible for carrying out necessary technical work to support PPSP.

One issue being addressed in the relicensing process is the adequacy of the oxygen content of water being released through the dam's turbines. Fish kills below the dam have occurred in the past due to low oxygen levels. Within the Conowingo Reservoir, the oxygen content of water in deep layers declines during summer months. When dam releases occur, water is often discharged from these layers of water low in dissolved oxygen (DO).

To examine the DO problems at the Conowingo facility and explore various means of alleviating those problems, Martin Marietta has undertaken development of a series of simulation models of the major components of the reservoir-river system. Three compartments of the system are being modeled: 1) oxygen dynamics of the reservoir ecosystem, 2) the pattern of water withdrawal from the reservoir under various dam operation regimes, and 3) the hydrology and oxygen dynamics of the river below the dam. In this report we describe a model developed for Item 2, the withdrawal of water from the reservoir.

A withdrawal model is needed as an interface between the river and reservoir models since DO and other water quality parameters are not uniformly distributed in the reservoir. That is, to determine the oxygen content of the water discharged from Conowingo Reservoir into the Susquehanna River below the dam, it is necessary to know the portions of the reservoir from which the water is being withdrawn. An additional question to be addressed is how withdrawal patterns change with variations in dam operation regimes.

The applicability of models described in the scientific literature for use at Conowingo are discussed in this report. Current meter data collected in the reservoir in 1981 are also described (Potera et al., 1982), and an empirical and statistical method for describing water withdrawal from the reservoir are presented. Results of dye transport studies done in conjunction with the current meter studies are presented in Appendix B, and are addressed as support for the conclusions drawn from analysis of the current meter data.

A.II. EVALUATION OF EXISTING WITHDRAWAL MODELS

Two withdrawal models described in the literature were considered to have potential applicability to Conowingo Reservoir: the Debler-Craya model (Debler 1959) and the Waterways Experimental Station (WES) model (Bohan and Grace, 1973). These two models were also representative of most of the models available in the literature. The suitability of these models was assessed before any attempts were made to develop an empirical and statistical model based on continuous current meter, temperature, and dye-transport data taken in the reservoir.

The Debler-Craya and the Waterways Experimental Station withdrawal models share a number of characteristics. Both determine the thickness of the withdrawal zone from the density gradients in the reservoir, the discharge rate from the reservoir, and the physical characteristics of the dam, e.g., height, width, location, and size of outlet; both also consider only vertical differences in velocity and do not deal with horizontal variations.

One characteristic specific to the Debler-Craya method is that it assumes a uniform velocity over the depths from which water is withdrawn, while assuming zero velocities at other depths. Current-meter data collected in 1981 (see Section A.III) indicated that this type of extreme flow stratification did not occur over the range of temperature gradients that are observed in Conowingo Reservoir. Thus, this method was considered inappropriate for use.

The WES method establishes the depth of maximum velocity within the withdrawal zone based on the location of the outlet and the thickness of the withdrawal zone. The distribution of velocities within the withdrawal zone is then determined from the density gradient and the vertical distance from the point of maximum velocity. The distribution of velocities, as calculated using this method, is more similar to that observed in Conowingo Reservoir than in the case of the Debler-Craya approach. However, for any given density gradient, the relative magnitudes of the velocities determined by the WES method at different depths will not change with changes in discharge, i.e., the shape of the velocity profile will remain constant, with magnitude of all values changing the same amount. Time-series plots of the current meter data indicate that the relative magnitudes of velocities at different depths do in fact change in response to changes in dam discharge during time periods when the density gradient does not change. Thus, this basic characteristic of

the WES model is inappropriate to the Conowingo Reservoir. Another relevant characteristic of the WES model is that it will predict no change in the proportions of the velocities at various depths, even if the magnitude of the density gradient does change, so long as the gradient remains linear. This model was developed for use in "normal" lake situations, where a steep thermocline exists between relatively homogeneous warm surface and cool deep layers. Conowingo Reservoir does not exhibit strong density stratification and typically has very small temperature differences between the top and bottom layers of the reservoir. The temperature gradient is accurately described by the temperature difference between the recorders at 10 m and 20 m (Fig. A-1). The gradient has been confirmed with numerous surface-to-bottom temperature profiles (Martin Marietta, unpublished data in PPSP database; not shown). Temperature gradients are rarely more than 2°C from surface to 24 m depth, and profiles of dissolved and suspended material (except for DO) never show any stratification, and thus do not contribute to density gradients.

To supplement the continuous data, discrete temperature profiles (at 2 m intervals for 25 separate days, with dawn-to-dusk series on 8 days) were taken at a station 140 m upstream of the turbines. The data indicated that almost all of the profiles were approximately linear, except for diel warming/cooling of the top 3 m layer. Below this 3 m layer, the profiles were invariant even though dam discharge varied from 0 to 46,000 cfs during the period. These discrete observations substantiated the assumption of weak linear density gradient persisting over most of the summer in the reservoir.

Because the WES method has been successfully applied to a number of reservoirs, we attempted to apply it to the estimation of water withdrawal from Conowingo Reservoir, in spite of its apparent drawbacks. Specifically, we calculated vertical velocity profiles (from temperature measurements every 2 m) using the WES method (Bohan and Grace 1973), and compared the estimated current profiles to current velocities measured at three depths. The comparisons were made for eleven separate time periods during the summer of 1981. Those periods were characterized by the greatest thermal stratification observed during intensive monitoring of the reservoir in 1981, and covered a range of turbine withdrawal rates from zero to 47,000 cfs. None of the current velocity profiles estimated by the WES method showed shapes like the actual current measurements. In general, the profiles predicted by the WES method showed maximum velocities over a broad depth range, with reduced velocities occurring only very near the surface or the bottom. Those profiles showed no apparent variation with discharge. In contrast, actual current profiles showed maximum velocities near the bottom and minima near the surface. The steepness of this velocity gradient decreased with increasing discharge.

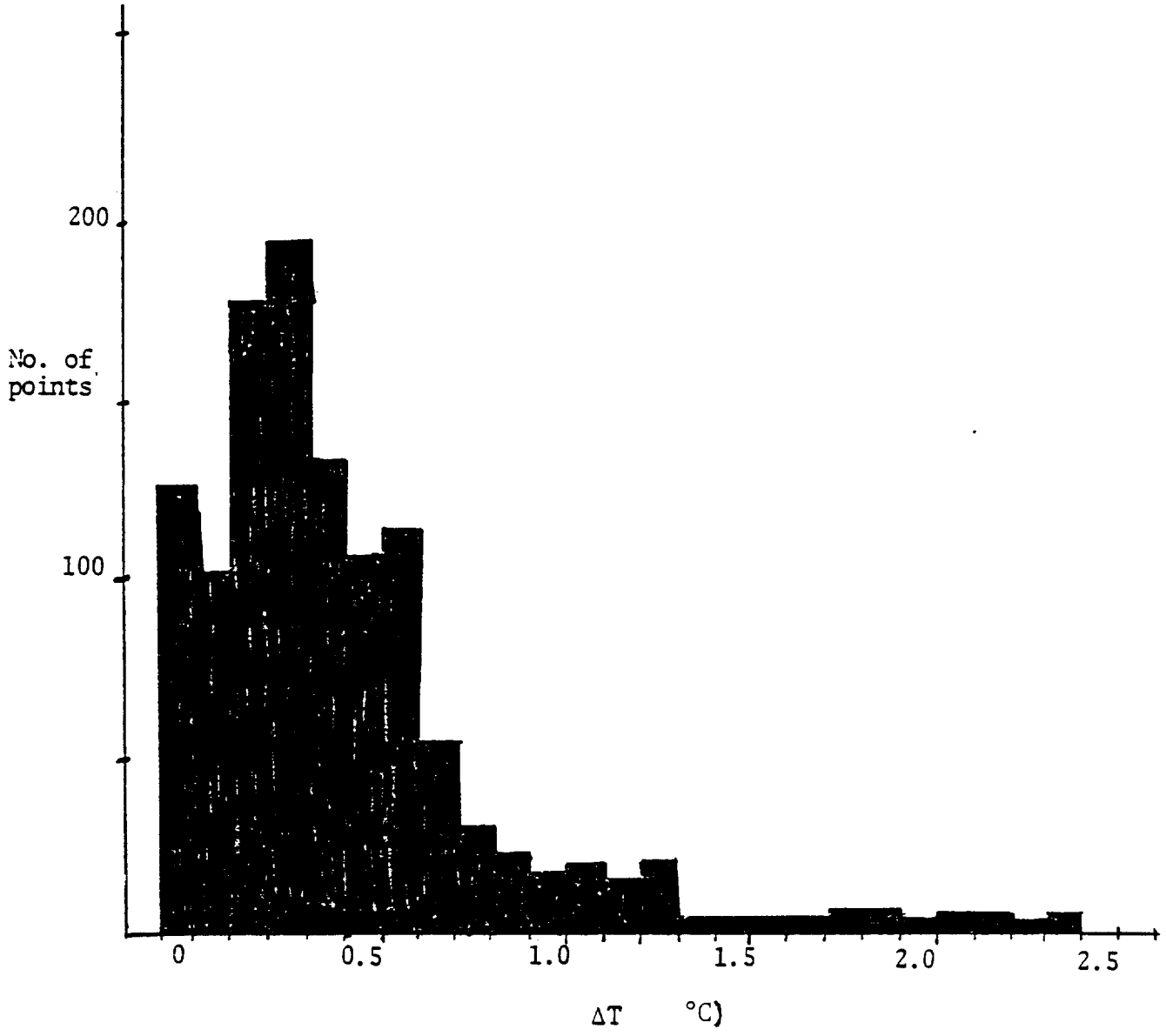

Figure A-1. Frequency of temperature difference, in degrees, between depths of 10-20 m, 12 July 1981 to 18 August 1981.

The differences between actual velocity profiles and those predicted by the WES method, and the inability of velocity profiles estimated by the WES method to change shape with discharge, indicated that the WES method would not accurately estimate water withdrawal from Conowingo Reservoir. The reasons for the lack of fit of estimates using the WES method to measure currents have not been identified. Possibly, the weakly stratified conditions in the reservoir may be beyond the range of conditions used to develop the WES method. Local withdrawal near Conowingo Dam may be influenced more by local reservoir geometry or bottom friction than by the vertical density gradient

As an alternative to the WES method, the extensive current meter data were used to develop an empirical model of water withdrawal. The development of this empirical withdrawal model is presented in the remainder of this appendix.

A.III. EMPIRICAL MODEL

Because of the inapplicability of the Debler-Craya and WES existing withdrawal models, we examined current-meter data collected in 1981 to determine the feasibility of developing an empirical withdrawal model for Conowingo based on statistical relationships between current velocity patterns and dam discharge patterns.

The empirical model that we developed determines velocity fields under different discharge conditions, along a plane parallel to the face of the dam and located 140 m upstream from the dam. Figure A-2 shows the location of that plane (Transect 1) in the reservoir. Velocity fields characterized for different discharges may be used to define the manner in which different discharge rates affect the pattern of water withdrawal. This withdrawal model is intended to be used in conjunction with the oxygen dynamics model being developed for the reservoir. That model considers the reservoir as having two layers. The velocity fields developed in this withdrawal model can be divided into segments that correspond to the layers in the reservoir model and will serve to determine the proportion of water that is withdrawn from each layer under different operating regimes. The data used in characterizing the velocity fields are described below.

A. AVAILABLE DATA

Velocity data were collected during the summer of 1981 using an array of continuously recording current meters deployed at two or three depths at four stations along a transect 140 m upstream of the dam. Endeco Model 105 and Braincon Model 1381 current meters were used. The manufacturers' specifications for these instruments state that the threshold of detection for both the Endeco and Braincon units is 2.4 cm/sec. For most of the meters, the observed operational thresholds (based on the 1981 data) were in the range of 1 to 1.6 cm/sec. The locations of the ten current meters in the withdrawal plane as shown in Fig. A-3.

Also shown are the corresponding locations of the intakes for the dam turbines and of continuous DO and temperature meters deployed in the plane of the velocity field. The width of the reservoir at Transect 1 is approximately 1350 m, much greater than the distance over which the meters were deployed.

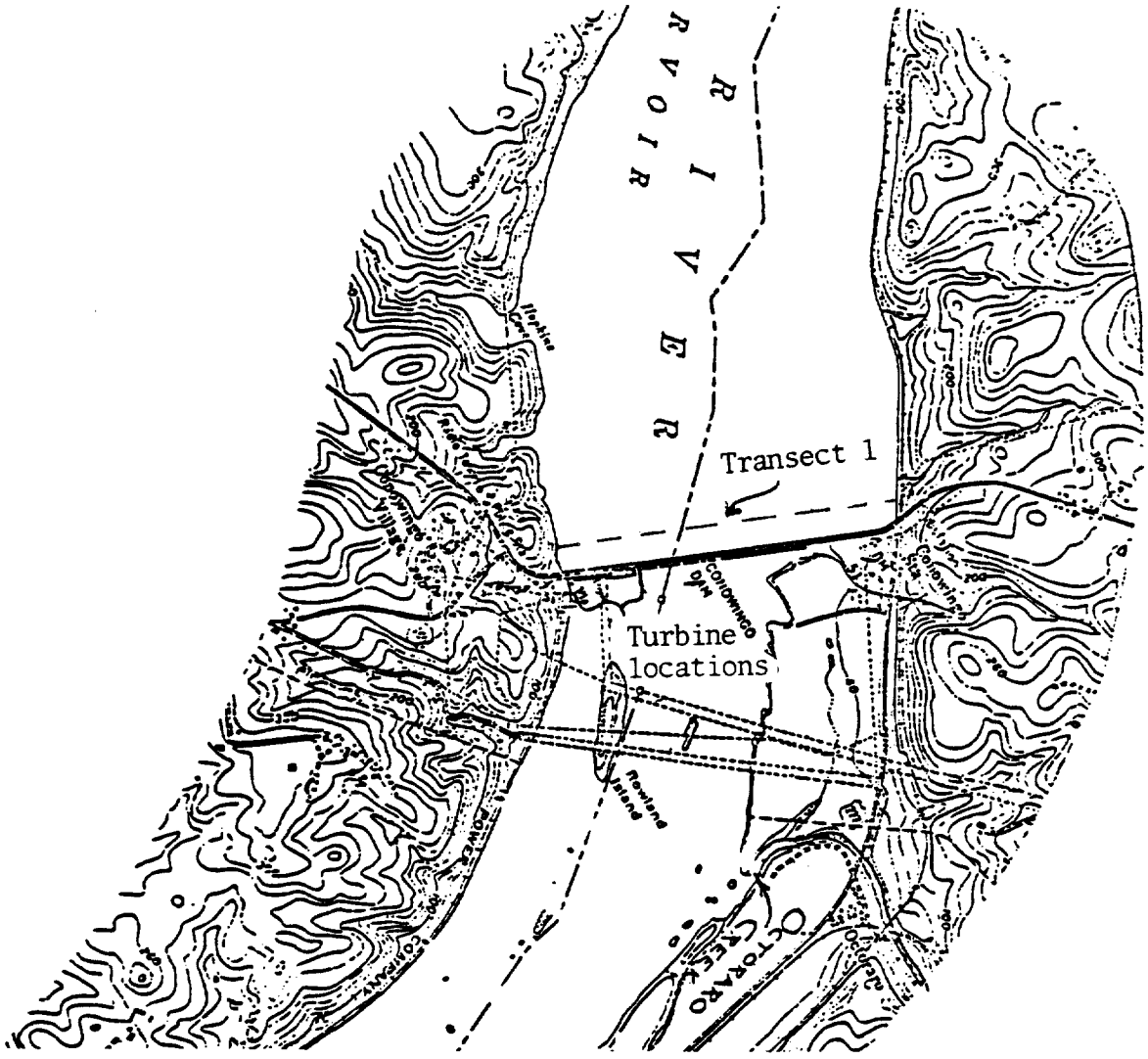

Figure A-2. The location of Transect 1 in Conowingo Reservoir. The transect is 140 m above the dam. The turbines are located on the left side of the dam.

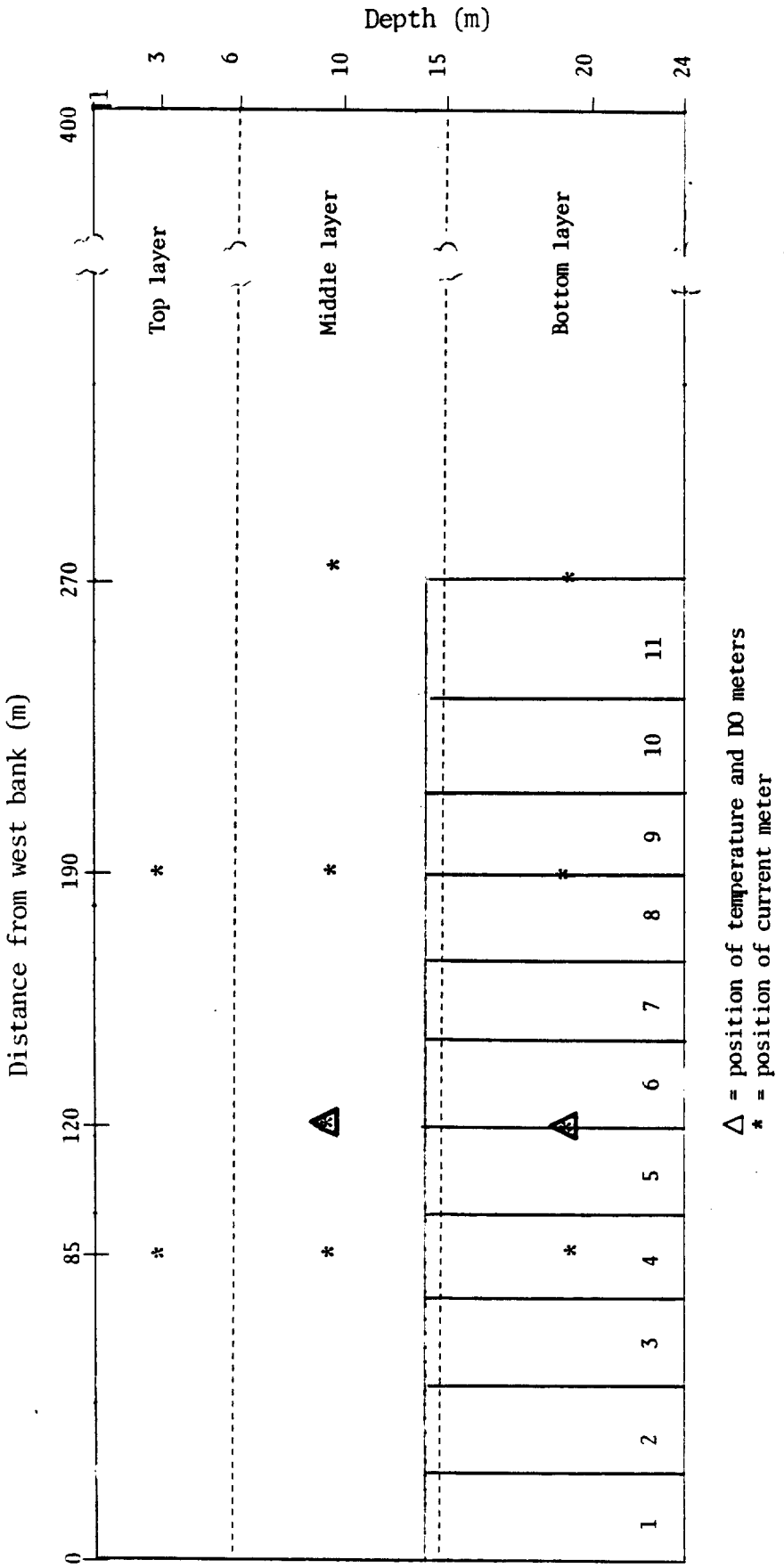

Figure A-3. Approximate positions of current, DO, and temperature meters at Transect 1 and relative positions of the eleven turbines in Conowingo Dam.

The meters were positioned within the region of the turbine intakes because this was assumed to be the location where velocities would be strongest and thus more readily measured. Separation of velocity signals from noise in current meter data is very difficult when velocities are low.

Figure A-4 shows the times during which each continuous-current, DO, and temperature meters were deployed and recording. Only two current meters were believed to still be recording accurately after 13 August. A USGS gage below the dam was the source of water height records which were converted to discharge from the dam. Records of turbine operating conditions were obtained from PECO. All the data taken prior to 13 August were used in the analyses. Data taken after 13 August was not used due to possible inaccuracies in the data.

B. DATA REDUCTION

Data analysis necessary for development of a withdrawal model required reduction of the raw current-meter data. Current meter velocity data were broken down into two components, one parallel to the face of the dam, and the second perpendicular to the dam face. The latter vector component was then used to calculate flux of water from a given layer of the reservoir as a function of discharge volume.

One alternative to the use of the perpendicular component for developing the withdrawal model, use of the component of velocity in the direction of strongest flow, was considered and rejected. The difference between the two approaches is that use of the perpendicular component assumes a withdrawal surface parallel to the dam face, while use of the strongest flow component assumes a curved withdrawal surface, the shape of which is defined by the components themselves and is dependent on the combination of turbines operating at any given time. Figure A-5 lists the frequencies of use (more than 10 hours) of various combinations of the eleven turbines during the summer of 1981. The direction of strongest flow under a particular turbine combination regime was determined for each meter by taking the data collected under that regime and regressing the component of the velocity parallel to the dam on the component of the velocity perpendicular to the dam. The slope of the regression line represents the tangent of the angle for the direction of strongest flow.

For many of the operating conditions, there were no velocity data from some of the meters and a small number of observations at the others. For some locations and operating conditions for which data were available, there were some variations in the angle of flow of the various meters under any given turbine

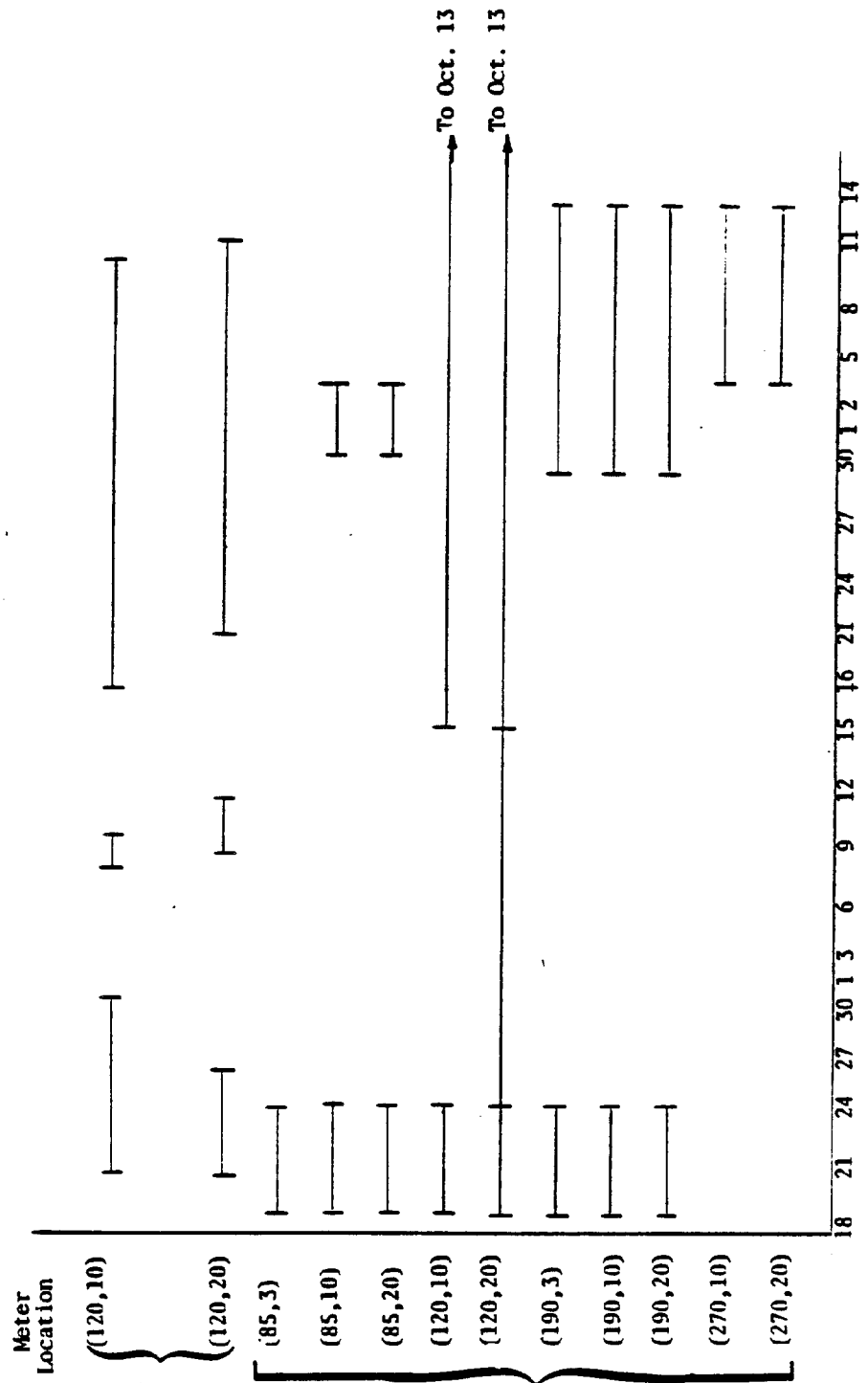

Figure A-4. Data record for temperature and current meters. The solid lines indicate the times during which the meters were deployed and recording correctly.

Turbines On											Frequency (hr)
1	2	3	4	5	6	7	8	9	10	11	
			NONE								1222
				X							426
	X										157
X	X	X	X	X	X	X	X	X		X	88
				X	X						82
X											56
					X						56
X	X			X	X		X	X		X	43
							X				42
X	X			X	X						42
X	X										35
						X					26
X	X	X	X	X	X	X	X	X	X	X	25
X	X	X	X	X	X		X	X		X	22
X	X			X	X		X			X	19
X	X		X	X	X	X					19
		X	X	X	X		X		X		16
		X	X	X	X		X	X	X		15
X	X			X	X		X				15
			X	X	X	X					15
X		X	X	X	X	X	X	X		X	14
			X	X	X	X	X	X	X		14
				X	X		X				13
	X			X							12
			X	X	X	X	X				12
X	X	X		X	X	X	X	X		X	12
X				X							11
X			X	X	X						11
		X		X	X	X					11
		X		X	X	X	X				11
X	X		X	X	X	X	X	X	X		11
		X	X	X	X		X	X			10
											2183 ≈ 76% of operating time

Figure A-5. Frequency of use (hr) for all turnbine combinations operating more than 10 hours from 17 June to 15 October, 1981.

combination. However, these angular variations were generally on the order of 30° or less. We concluded that the variations were still too large to determine the direction of strongest flow for all current-meter locations, as a function of which turbines were operating.

C. REGRESSIONS OF VELOCITY VS DISCHARGE

The overall objective of these analyses was to describe how the vertical velocity field changed as a function of discharge. The first step in this procedure was to determine the relationship between dam discharge and the component of the velocity perpendicular to the dam for each current meter. (Henceforth the word velocity means the component of the velocity perpendicular to the dam.) Both linear and non-linear regressions were tried; linear regressions gave the better fit.

Data points used in the regressions were those recorded when flow (i.e., dam discharge) was within 10 percent of the flow at the previous hour so that velocities at times of rapidly changing flow were not used in the regressions. Such transitional values would have increased variability within the data sets. A point [velocity (T), flow (T)] was used in the regression if:

$$\left| \frac{\text{Flow (T)} - \text{Flow (T-1)}}{\text{Flow (T)}} \right| < .10 \qquad \text{(A.1)}$$

where T = time (hr).

Figure A-6 shows the linear regression lines for the current meters at locations (120,10) and (270,20). These locations had the highest and the lowest correlation coefficients (0.943, 0.723, respectively), indicating the range of fit for all of the current meters. Table A-1 lists the regression lines for each of the ten meters.

Ideally, it would have been preferrable to perform regressions using only data from periods when steady state was reached in velocity at the location of the current meters after the discharge at the dam reached a steady state. At high flows most of the velocity points did satisfy such a 10% criterion (Eq. A.1), whereas at low flow most did not. This suggested that at lower flows the velocities take longer to reach an approximate steady state and also may have reflected the poor

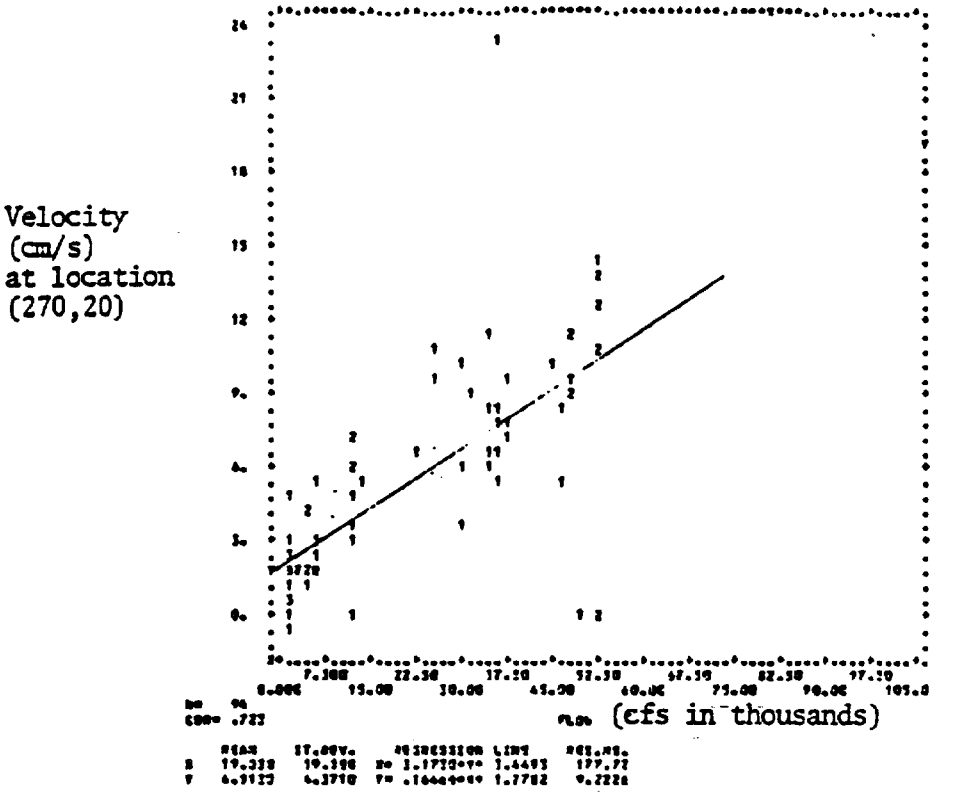

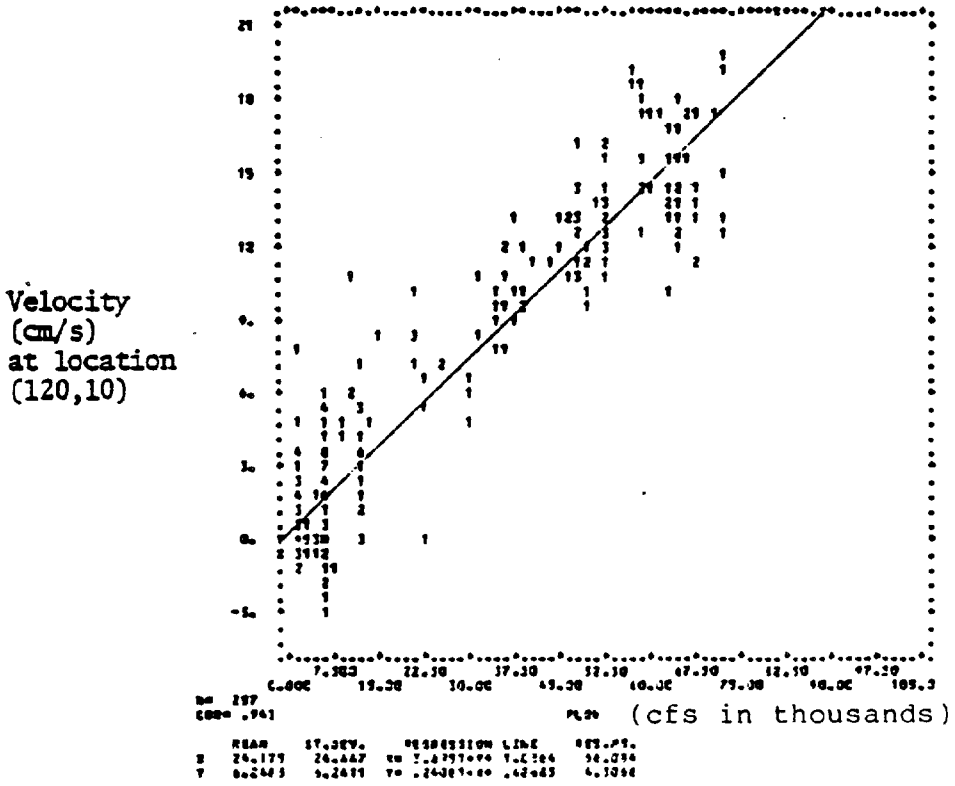

Figure A-6. Linear regressions of flow on velocity for meters at locations (270,20) and (120,20).

Table A-1. The regression functions of velocity on flow for the ten current meters and their correlation coefficients

Location of Meter: Distance from West Bank, Depth from Surface (m)	Equation[a]	Correlation Coefficient
(85,3)	Velocity = 0.286 * Flow - 0.242	0.884
(85,10)	Velocity = 0.274 * Flow + 0.100	0.934
(85,20)	Velocity = 0.265 * Flow + 0.995	0.906
(120,10)	Velocity = 0.241 * Flow + 0.427	0.943
(120,20)	Velocity = 0.196 * Flow + 2.140	0.925
(190,3)	Velocity = 0.239 * Flow + 0.671	0.830
(190,10)	Velocity = 0.234 * Flow + 0.742	0.893
(190,20)	Velocity = 0.218 * Flow + 1.788	0.783
(270,10)	Velocity = 0.176 * Flow + 1.319	0.774
(270,20)	Velocity = 0.165 * Flow + 1.778	0.723

[a] Velocity in cm/s; flow in cfs * 10^{-3} (cfs in thousands)

signal to noise ratio in current meter data at low flows. When all 10 velocity time-series were examined to determine periods when they simultaneously satisfied the 10% criterion, the number of data points retained was too small to carry out regression analysis. Accordingly, regressions were done independently on the steady-state velocity data from each current meter, irrespective of whether the remaining current meters were at steady state.

The velocity field for any specified discharge rate is established by reading the velocity for each meter at that rate from the regression lines. These composite velocity fields for six dam discharge rates (3,000, 5,000, 10,000, 20,000, 40,000 and 70,000 cfs) are shown in Fig. A-7. The predicted velocities are indicated in the approximate locations of the current meters in the velocity field.

Confidence intervals were calculated for both the mean of the velocities and an individual velocity for the six flows for each of the 10 regression lines (Table A-2). For each meter, the six confidence intervals were made with a simultaneous confidence level of 95%.

A major concern was the need to estimate velocities near the detection limits of the current meters (i.e., at velocities expected under feasible minimum discharge conditions). The intent of our regression analyses was not to characterize every situation, but to define long-term average withdrawal patterns as functions of dam discharge. We expected day-to-day variations in flow to generate noise in the long-term current meter data. Continuous current meters (rather than discrete measurements) were used to acquire long-term data from which a flow pattern could be detected in spite of noise contaminating individual observations of velocity. The confidence intervals about individual point estimates of velocity do overlap. However, all of the regressions revealed significant relationships between discharge and velocity. Thus, a point on each regression line is the best estimate of velocity for any given discharge, given the entire data set covering a wide range of discharges.

Based on the point estimates (from the regressions) of velocities for each meter at various discharges (Fig. A-7), the bottom layer velocities are always above the practical detection limit of the current meters. Point estimates for velocities in the upper two layers fall below this detection limit only for discharges of 3000 and 5000 cfs. The velocities in that region at those flow levels may not be detectably different from zero. However, if one were to make the assumption that the surface layers are, in fact, stagnant at low flows, then the general pattern defined by the analyses is accentuated -- most of the water must be withdrawn from the bottom layer at low discharges, and more surface water is mixed in as discharge increases.

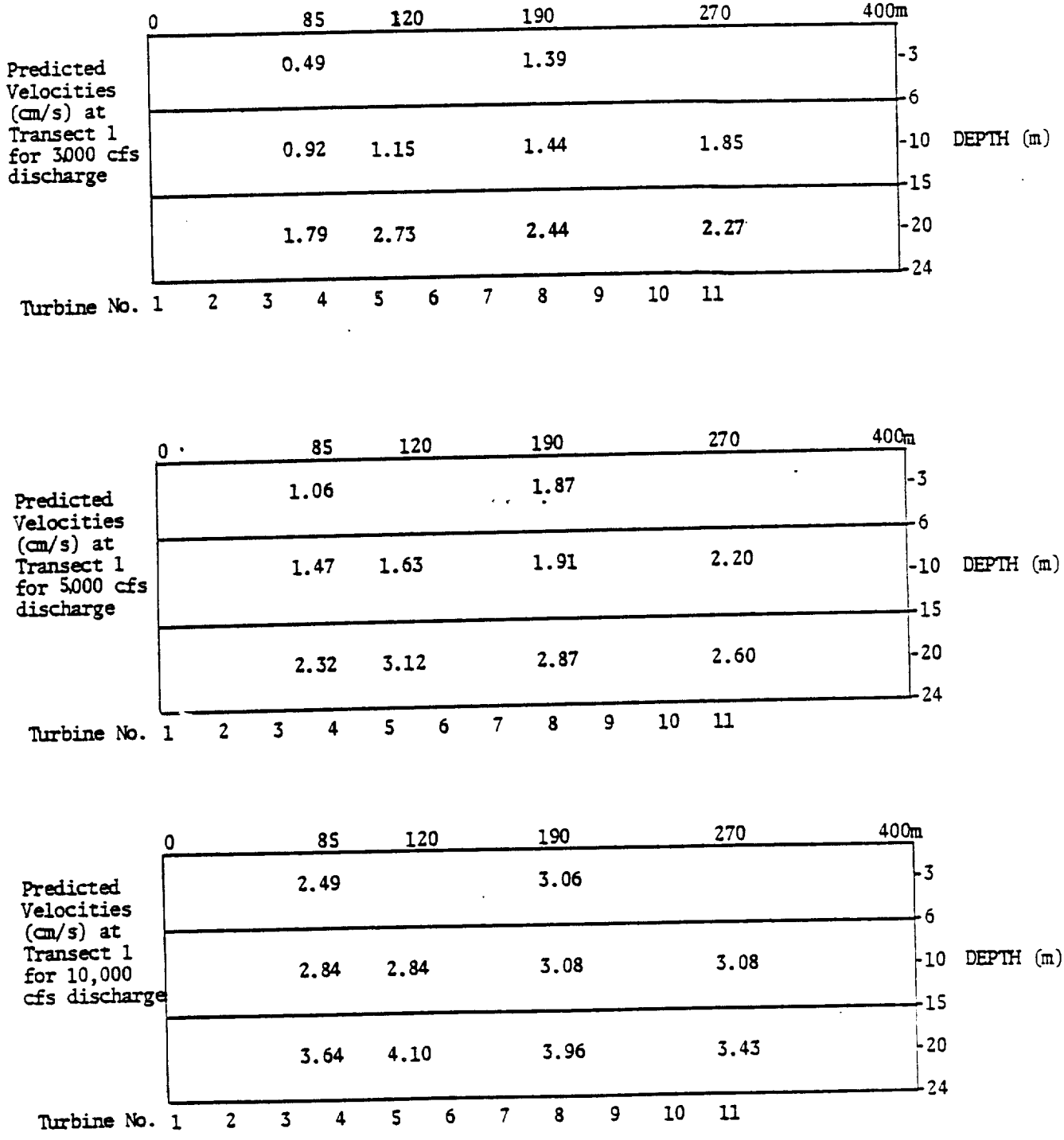

Figure A-7. Predicted velocities in the withdrawal surface (facing upstream at the dam) for 6 different discharge rates. Numbers 1 through 11 indicate the horizontal position of the turbines in the dam, and numbers at the top of the diagram represent distances from the west bank of the reservoir.

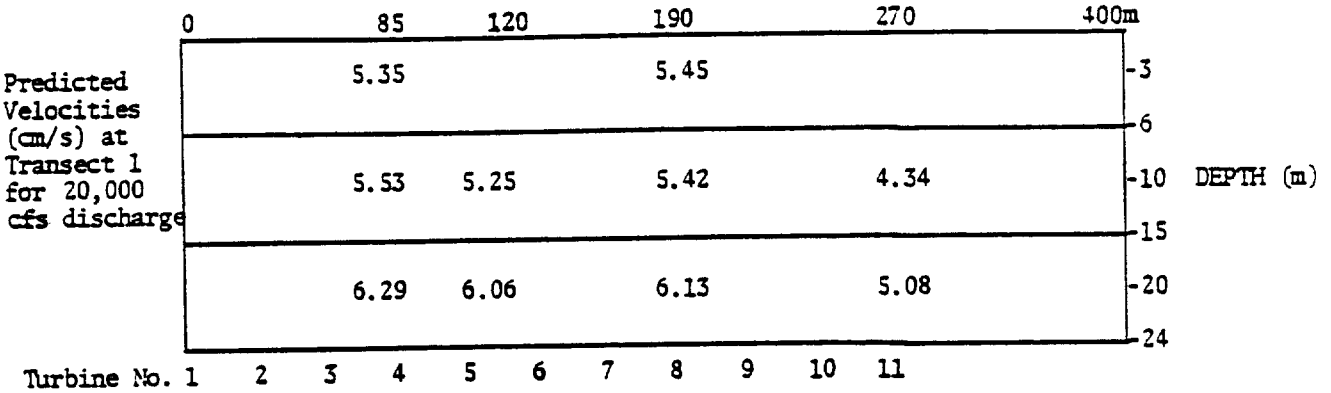

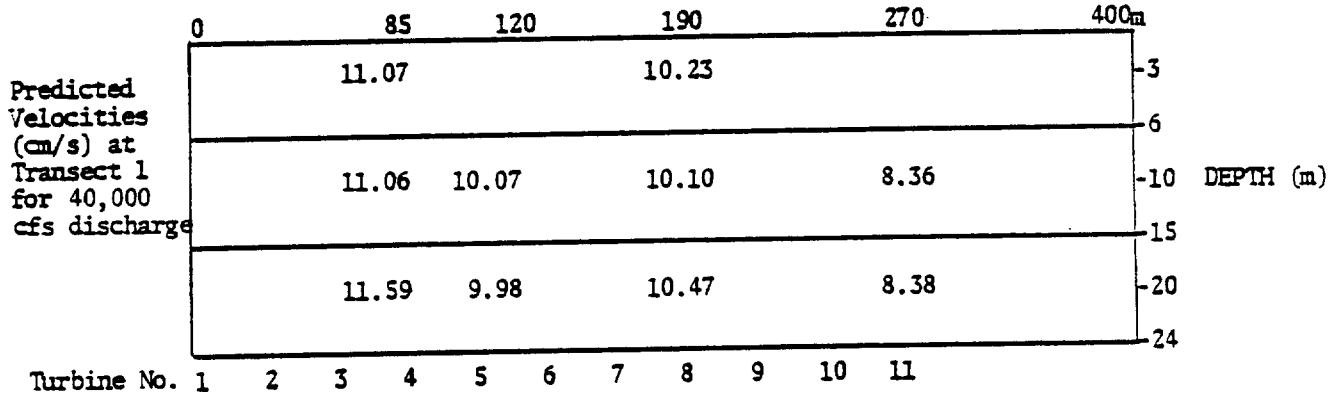

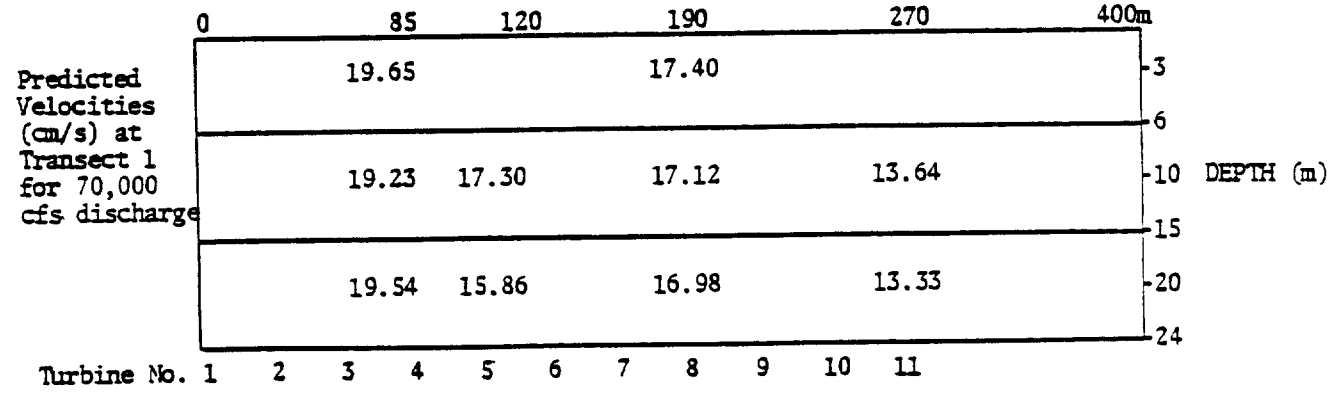

Figure A-7. Continued.

To confirm current velocity estimates at low discharges that were derived from the regressions, a number of discrete dye release experiments were performed at discharges of 3000, 5000 and 8000 cfs. The results of these time-of-travel experiments are described in Appendix B.

D. EFFECTS OF STRATIFIED FLOW ON VELOCITY FIELDS

The data set used for the linear regressions covered periods of both stratified and unstratified flow. To find out if the velocity fields determined using these linear regressions adequately represented velocities during both stratified and unstratified flow, the Froude number (Yih, 1965) was calculated for each data point (velocity, flow) for which temperature data at two depths was also available.

Flow was considered to be stratified if the Froude number was less than 0.32, based on work done by Yih (1965). The mathematical model of Yih described two-dimensional flow towards a line sink whereas flow upstream of Conowingo Dam is a 3-dimensional system with a truncated line sink. However, Yih's theoretical model was the closest of those available in the literature to situations in Conowingo Reservoir. The Froude number is a function of the density gradient and the discharge as well as the physical characteristics of the withdrawal region in the dam and the reservoir. The density gradients in Conowingo Reservoir depended only on temperature differences in different depth layers (i.e., no stratification in dissolved or suspended material had been observed).

The Froude number was calculated from the following equation:

$$F = \frac{q}{D^2}\sqrt{\frac{Po}{G\beta}} \qquad (A.2)$$

where

- q = Q/W = volumetric discharge (per unit distance perpendicular to the plane of flow)
- Q = discharge (m^3/s)
- W = width of the discharge region = 270 m
- G = acceleration due to gravity = 9.8 m/s^2
- D = depth of the reservoir = 24 m

- Po = fluid density at the elevation of the orifice center line (kg/m^3)
- β = density gradient at the withdrawal location (kg/m^4)
- F = the Froude number.

The discharge from Conowingo Reservoir would have been stratified primarily at flows less than 20,000 cfs as indicated in Fig. A-8. No stratified flow occurred at flows above 24,000 cfs

Examination of the velocity fields (Fig. A-7) indicates that the predicted velocities over depth do become equal at or above 20,000 cfs. These results indicate that the linear regressions do produce velocity fields with the appropriate characteristics for both stratified and unstratified flow. Further refinement of the velocity fields was considered to be unnecessary.

E. PROPORTION OF FLOW FROM HORIZONTAL LAYERS

The velocity fields presented in Fig. A-7 were used to calculate the percent of the total discharge which comes from each of the horizontal layers under each discharge regime. These results are required for use of the reservoir model discussed in the introduction. To this end, the withdrawal surface was divided into three depth layers with thicknesses of six, nine, and nine meters for the top, middle, and bottom layers, respectively. The top layer roughly corresponds to the euphotic zone of the reservoir; a 6-m surface layer is also simulated by the reservoir model. The bottom layer covers the vertical extent of the turbine penstocks (Fig. A-3). The middle layer covers the 9-m of the water column between the top and bottom layers. The current meters were situated approximately at the middle of each layer (Fig. A-3). Withdrawal from three layers was estimated as an aid in understanding the dynamics of flow near the intake. It was later necessary to combine the middle and bottom layers in order to maintain consistency with the two-layered reservoir model.

To determine the percent of the flow coming from each of the layers under any given discharge rate, the average velocity in each layer was multiplied by the depth of the layer and divided by the sum of the products of the average velocities and the depths of the three layers.

$$P_i = \frac{V_i \times D_i}{\sum_{i=1}^{3} V_i * D_i} \qquad (A.3)$$

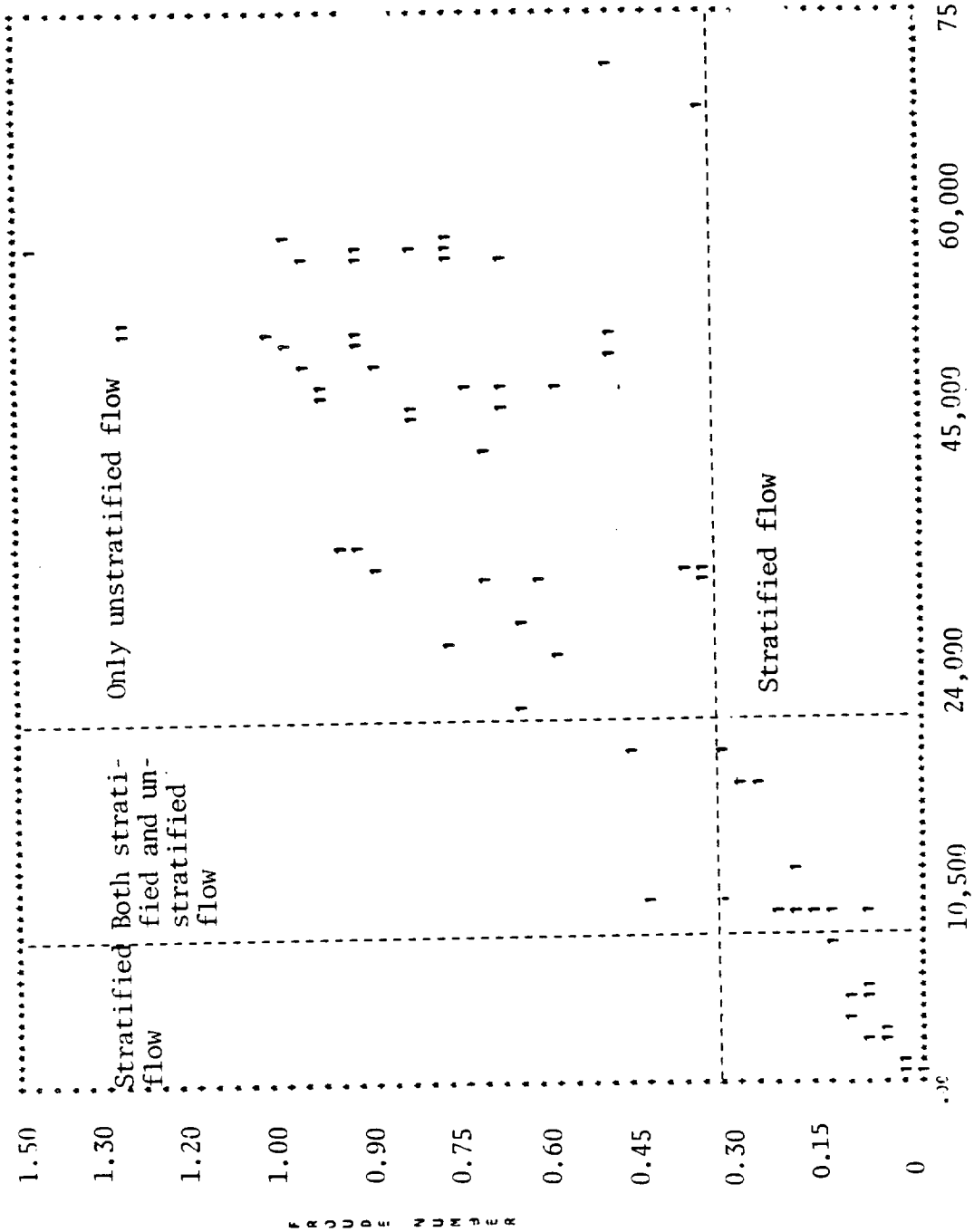

Figure A-8. Froude numbers calculated at all discharges when suitable temperature data were available; discharges at which stratified and unstratified flow would occur are indicated.

where

P_i = percent of the flow being withdrawn from layer i

V_i = average velocity in layer i (m/s)

D_i = thickness of layer i (m).

The percent of the discharge coming from the three layers is graphed in Fig. A-9 as a function of discharge. At high flows, the percent of the discharge coming from each layer is approximately equal to the percent of the total depth contained in that layer, whereas at low flows more water is coming from the bottom layer and less from the top layer.

The 95% confidence intervals for the mean velocities for each meter for each flow (Table A-2) suggest that the predicted proportion of flow from each layer are poorest (i.e., have the greatest likelihood of inaccuracy) at low discharge rates (i.e., 10,000 cfs and less).

Table A-2. Simultaneous confidence intervals for velocity at the 95% level at 6 different flows for each of the ten current meters. Confidence intervals are given for both the population mean and an individual value.

Current Meter Flow (cfs)	Confidence Intervals for Velocity (cm/s) The Population Mean	An Individual Point
(85,3)		
3000	-1.40 - 2.37	-10.68 - 11.65
5000	-0.76 - 2.88	-10.10 - 12.21
10000	0.32 - 4.15	- 8.64 - 13.61
20000	3.95 - 6.73	- 5.75 - 16.43
40000	9.85 - 12.25	- 0.01 - 22.12
70000	17.73 - 21.51	8.46 - 30.78
(85,10)		
3000	-0.39 - 2.24	- 6.35 - 8.70
5000	0.20 - 2.74	- 6.30 - 9.24
10000	1.68 - 4.00	- 4.91 - 10.59
20000	4.61 - 6.55	- 2.14 - 13.31
40000	10.23 - 11.90	3.35 - 18.77
70000	17.97 - 20.60	11.51 - 27.06
(85,20)		
3000	0.24 - 3.34	- 7.37 - 10.95
5000	0.83 - 3.81	- 6.83 - 11.47
10000	2.28 - 5.01	- 5.48 - 12.77
20000	5.15 - 7.44	- 2.80 - 15.39
40000	10.61 - 12.58	2.52 - 20.67
70000	17.99 - 21.09	10.39 - 28.70
(120,10)		
3000	0.73 - 1.57	- 4.26 - 6.56
5000	1.23 - 2.04	- 3.78 - 7.04
10000	2.47 - 3.20	- 2.58 - 8.25
20000	4.92 - 5.57	-.16 - 10.65
40000	9.68 - 10.44	4.65 - 15.47
70000	16.61 - 17.96	11.84 - 22.72
(120,20)		
3000	2.44 - 3.02	- 2.48 - 7.94
5000	2.34 - 3.40	- 2.09 - 8.33
10000	3.35 - 4.36	- 1.11 - 9.31
20000	5.34 - 6.29	.86 - 11.27
40000	9.73 - 10.24	4.78 - 15.19
70000	15.41 - 16.33	10.65 - 21.09

Table A-2. Continued.

Current Meter Flow (cfs)	Confidence Intervals for Velocity (cm/s) The Population Mean	An Individual Point
(190,3)		
3000	.28 - 2.50	- 9.22 - 12.00
5000	.30 - 2.93	- 8.74 - 12.47
10000	2.09 - 4.03	- 7.54 - 13.66
20000	4.61 - 6.28	- 5.14 - 16.03
40000	9.32 - 11.12	-.37 - 20.31
70000	15.80 - 18.96	6.71 - 28.05
(190,10)		
3000	.64 - 2.25	- 6.27 - 9.16
5000	1.14 - 2.68	- 5.80 - 9.62
10000	2.38 - 3.73	- 4.62 - 10.78
20000	4.82 - 6.02	- 2.27 - 13.12
40000	9.46 - 10.75	2.40 - 17.80
70000	15.98 - 18.26	9.37 - 24.88
(190,20)		
3000	1.27 - 3.61	- 8.84 - 13.72
5000	1.75 - 4.00	- 8.41 - 14.15
10000	2.93 - 4.93	- 7.31 - 15.22
20000	5.25 - 7.00	- 5.13 - 17.38
40000	9.52 - 11.40	-.80 - 21.72
70000	15.30 - 18.62	5.62 - 28.31
(270,10)		
3000	.86 - 2.83	- 5.52 - 9.22
5000	1.26 - 3.13	- 5.17 - 9.56
10000	2.24 - 3.91	- 4.28 - 10.43
20000	4.08 - 5.59	- 2.51 - 12.17
40000	7.23 - 9.46	.96 - 15.73
70000	11.47 - 15.76	6.00 - 21.23
(270,20)		
3000	1.20 - 3.35	- 5.79 - 10.34
5000	1.58 - 3.62	- 5.46 - 10.66
10000	2.51 - 4.34	- 4.62 - 11.47
20000	4.25 - 5.90	- 2.96 - 13.11
40000	7.14 - 9.59	.28 - 16.45
70000	10.95 - 15.66	4.97 - 21.64

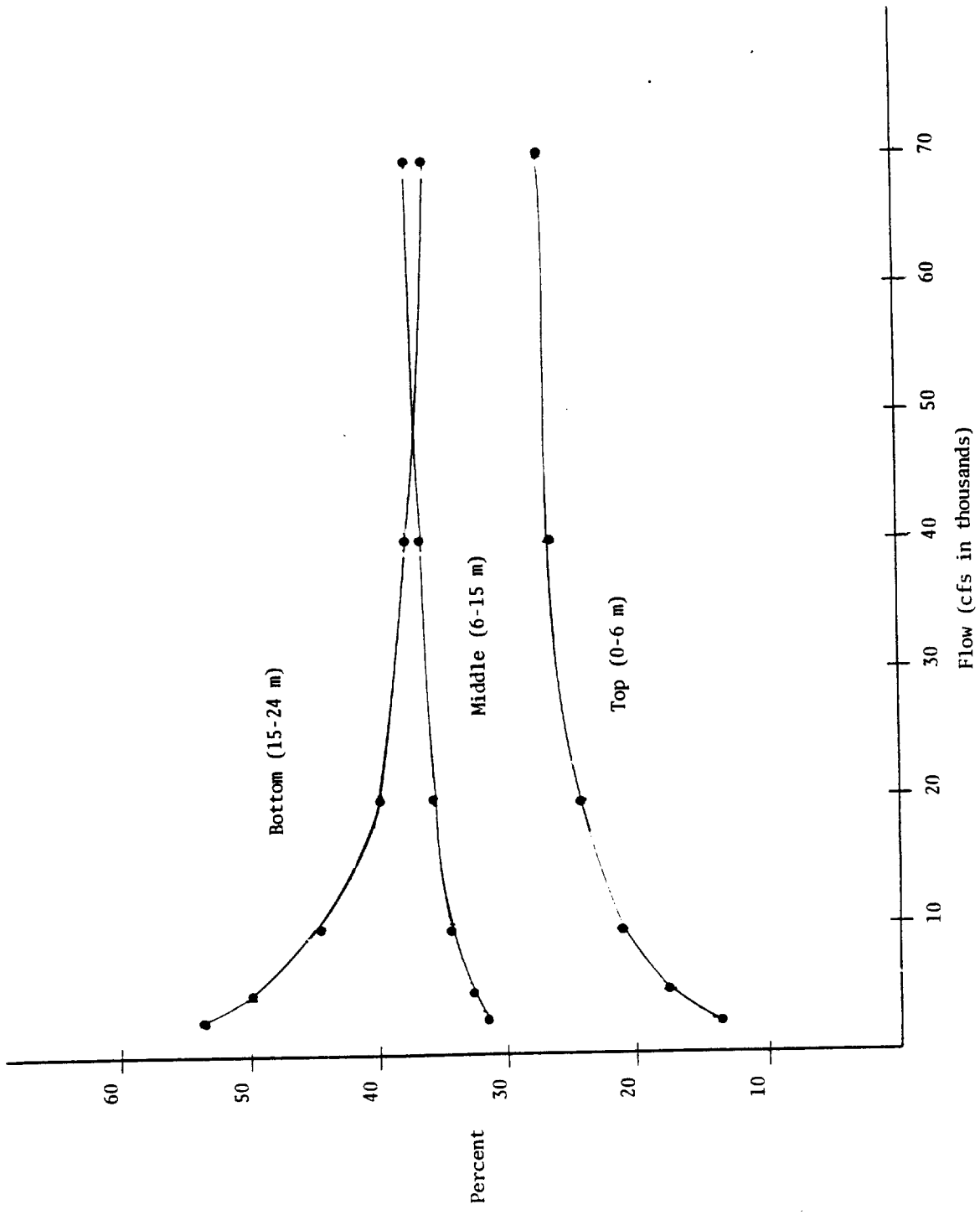

Figure A-9. Percent of water being withdrawn from the top, middle, and bottom layers of the reservoir.

A.IV. DISCUSSION

The major characteristic of withdrawal patterns observed at Conowingo is that water tends to be drawn equally from all depths at high flows and selectively from the bottom layer at low flows. The findings presented in Figure A-9 wil be used in interfacing the withdrawal model with the reservoir model to examine the effects of various dam operation regimes on dissolved oxygen within the reservoir-river system.

It is evident that the point estimates of percent withdrawal from each layer are least reliable at low flows, which happen to be the flows most likely to be considered as potential minimum continuous flows. However, despite the variability inherent in these estimates of percentage withdrawal, the pattern shown as discharge increases is consistent: percentage from the bottom layer is high at low flows, and converges with percentage from the other layers as discharge increases. Thus, use of the point estimates plotted in Figure A-9 will provide reasonable representa tions of withdrawal patterns.

Several other uncertainties about the validity of the model can be raised relative to certain assumptions.

1) One such assumption is that the component of velocity perpendicular to the dam is adequate to represent actual water flux, as opposed to the velocity in the direction of strongest flow. The amount of data was inadequate to determine the angle of strongest flow for each of the many different turbine operating conditions, making the use of those angles impractical. For most of the turbine operating conditions and most of the meters the difference in angle between the direction of strongest flow and a line perpendicular to the dam was small since the plane of the velocity field was 140 m from the dam. The lack of suitable data merely prevented us from "fine tuning" the model and reducing the variability to some degree.

   Also, predicting the proportion of flow that comes from the horizontal layers of the reservoir is the most important use of this model. For a given vertical location (i.e., the location of one current meter string) the angles of strongest flow for the different depths tended to be very similar. Hence the proportion of flow from the different layers would not be changed by using component of velocity perpendicular to the dam

instead of that in the direction of strongest flow. Therefore, the use of the component of velocity perpendicular to the dam should not adversely affect the utility of the withdrawal model.

2) Another assumption is that the predicted velocities adequately determine the withdrawal patterns even though the width of the reservoir is much greater than the width of the region in which the current meters were deployed.

   The predicted velocities seem to adequately characterize the withdrawal patterns in front of the turbines, but are not sufficient to assess the velocities across the rest of the reservoir. However, if we assume that the proportions of the velocities from the different depth layers do not differ from those in front of the turbines, then the utility of the model for interfacing with the reservoir model is unaffected, since it is the percent of the discharge coming from each layer that is of interest. Hence we believe that the model does adequately describe withdrawal patterns.

Further substantiation of the current meter data analyses presented here comes from the results of the dye transport studies described in Appendix B. Although some discrepancies in velocities measured by the two techniques are evident, the pattern of selective withdrawal from the bottom layer at low flow is consistent between both studies.

APPENDIX B

WATER VELOCITIES AND WITHDRAWAL PATTERNS IN CONOWINGO RESERVOIR ESTIMATED FROM DYE TRANSPORT

Prepared By:

Robert L. Dwyer

B.I. INTRODUCTION

Vertical mixing and horizontal water movements in Conowingo Reservoir near the dam appear to be related to turbine operation (Philipp and Klose, 1981). Thus, information about currents near the turbine intakes at different discharge levels may suggest measures to improve the DO of the discharge. Data from the current meter arrays deployed in 1981 provided much information about these current patterns. However, the current-meter arrays had to be deployed 140 m from the dam to minimize the chance of encountering vertical velocity components. Consequently, current meters recorded only the initial speed and direction of water particles moving toward the intakes. No information on the trajectories of water particles would be obtained.

It was concluded that additional information about currents and mixing processes close to the intakes would be useful for verifying observations based on the current-meter data. Thus, to complement the information provided by current-meter data, ERM also performed dye tracer experiments during 1981 under controlled discharges of 3,000, 5,000, and 8,000 cfs. These discharges were considered feasible levels for a continuous minimum discharge. A detailed discussion of these experiments is presented by Potera et al. (1982).

Briefly, an individual dye release experiment consisted of the instantaneous release of a mass of dye at a single depth at a known distance from one or two turbines discharging at a controlled rate. The dye mass followed a current streamline toward the turbine intake, and dye concentration was measured at various points along the way. The following information can potentially be obtained:

- The travel time of the dye mass, divided by the linear distance between the release point and the turbine, provides an estimate of the integrated average speed of the water along the streamline. By locating release points close to the dam (where vertical components of velocity might interfere with current meter measurements), estimates of velocities near the intake can be obtained.

- An indication of how water from the dye release point contributes to the water discharged by the turbine is provided by time-series measurements of the dye from the turbine itself or from the tailrace. The peak dye concentration and the duration of the dye signal can be used to make a quantitative estimate of the dispersion and mixing of water from the layer in which dye was released with other reservoir layers.

- The shape of the current trajectory originating at a given dye release point can be determined if the progress of the dye mass can be monitored before it reaches the dam. These shapes yield information on phenomena such as current deflections (boundary effects) as water encounters the dam wall.

This appendix presents the results of Martin Marietta's analyses of the dye release data collected by ERM. The analyses were aimed primarily at estimating the relative withdrawal from different reservoir layers at low discharge levels, as corroboration of estimates derived from current-meter data. Other analyses of the dye data to estimate longitudinal dispersion near the turbine intakes have yet to be done.

B.II. METHODS

Detailed methods of the study are described by Potera et al. (1982). Turbine 5 was operated at 3,000 and 5,000 cfs, and turbines 5 and 6 were operated together at 8,000 cfs, for 5-hr periods on 10-12, 24, 25, and 31 August, and 1 September 1981. These turbine combinations provided a range of discharges which could feasibly be implemented as a minimum continuous discharge to alleviate water quality problems downstream of the dam. During each controlled discharge period, a number of pulses of Rhodamine WT dye were released at points on the withdrawal surface (i.e., at several depths at points directly upstream of the operating turbine as well as at points to either side of the axis of the turbines). Locations of all dye release points, as well as locations of current-meter arrays, are shown in Fig. B-1. These release points provided a two-dimensional picture of the influence on the pattern of water withdrawal of Turbines 5 and/or 6. Dye concentrations were monitored continuously at a number of ports connected to the intake and turbine structure, as well as discretely from grab samples taken between the release point and the intake, and from the tailrace boil of the turbine.

At first, dye releases were attempted at a number of distances from the dam, in order to select a distance which would yield a travel time long enough to permit collection of a number of discrete samples as the dye traveled to the intake. The optimum distance was determined to be 60-85 m from the dam. However, attempts to track individual dye pulses between the release point and Turbine 5 were largely unsuccessful, despite intensive sampling. It appeared that the dye release generally dispersed into a longitudinal stream with a cross-section of less than 1 m^2, making it very difficult to locate when sampling from a boat by lowering a hose connected to the fluorometer intake. Thus, it was not possible to ascertain the shape of the trajectories of individual dye releases. However, there were qualitative indications that water did not always travel a straight line (the shortest path) to the turbine intake. For instance, a number of surface releases of a different color dye (Fluorescein) were followed visually. These releases often followed curvilinear paths toward the dam, which did not fit the pattern of a simple converging flow field between the release point and the intake. Also, surface vortices were observed at 5,000 cfs at the dam above the two intake ports of Turbine 5, indicating that water traveled horizontally to the dam before converging at the surface above the intake.

Time-series dye data had to be reduced in order to calculate velocities. First, data for each release and sampling location were plotted as dye concentration vs time elapsed since release

(Fig. B-2 is an example; all plots are contained in Potera et al. (1982), Vol. II, Appendix C). The elapsed time of the peak dye concentration at the turbine is a measure of the average travel time of the dye pulse. Average velocity of a dye release was calculated as the straight-line distance between the release point and the turbine, divided by the elapsed time.

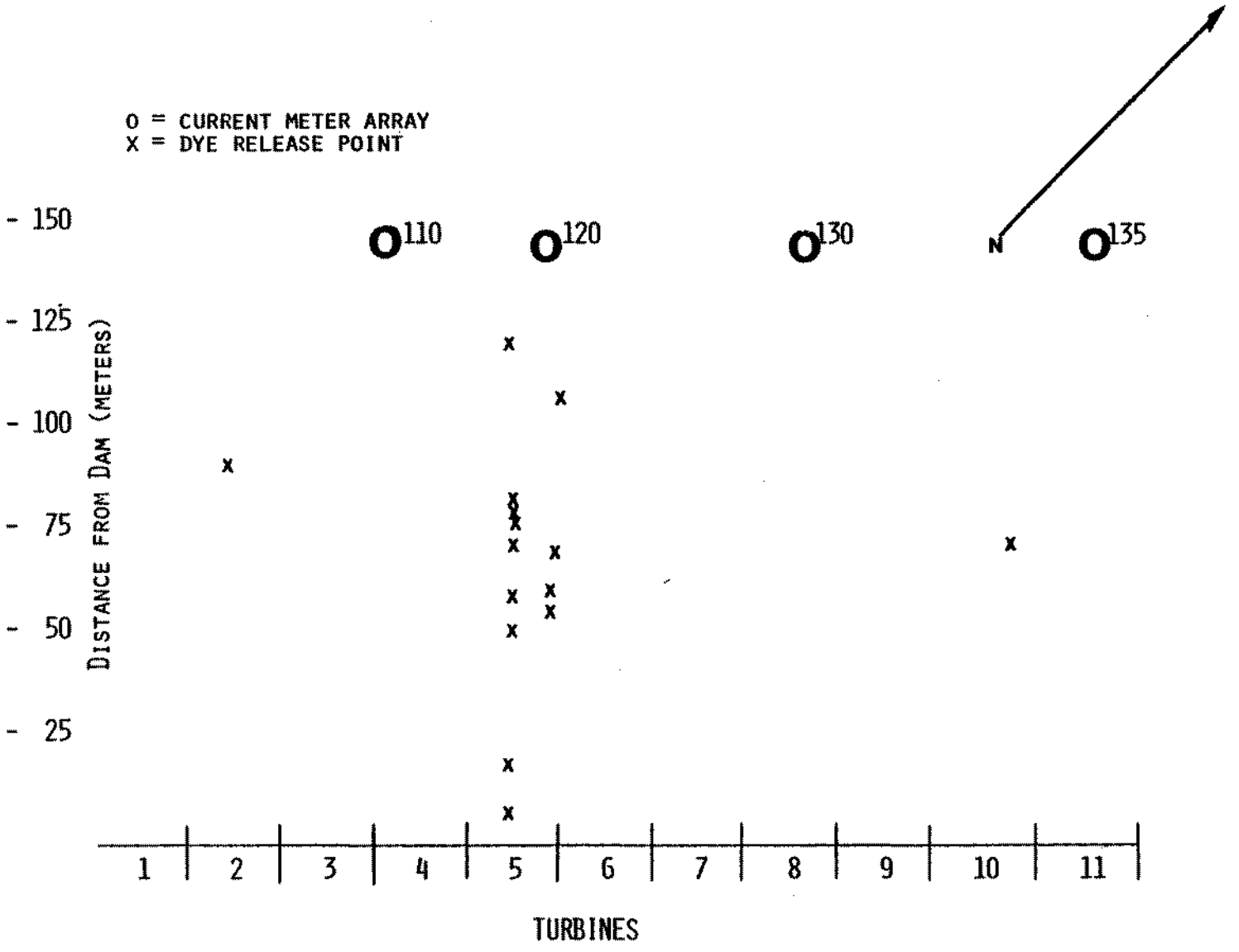

Figure B-1. Locations of dye releases and of current meter arrays, relative to turbines.

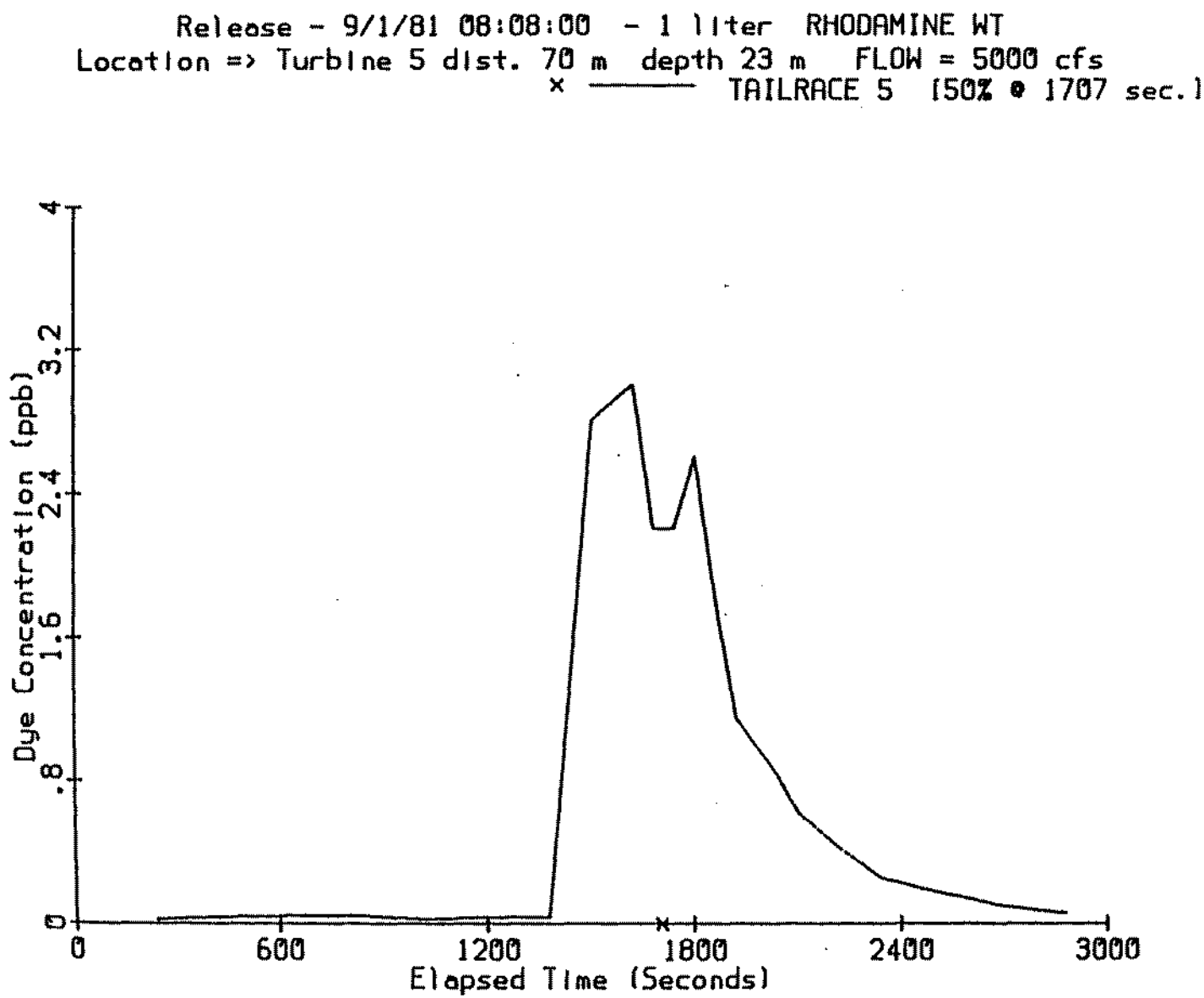

Figure B-2. Typical time series measurement of dye concentration in Tailrace vs elapsed time since release. (From Potera et al., 1982).

B.III. RESULTS

Velocities are listed in Table B-1, arranged by test discharge. The calculated velocities show considerable variation even between consecutive releases from the same location. These data are plotted by depth for each of the three test discharges in Figs. B-3, B-4, and B-5. Where more than one release was made, the mean velocity, and ± 1 Standard Error interval, are shown. Velocities for the 3,000 cfs discharge are largest near the bottom (18-20 m; Fig. B-3). For the 5,000 cfs discharge, velocities appear more evenly distributed over the water column (Fig. B-4). In contrast, velocities for the 8,000 cfs discharge appear to reach a maximum at mid-depth (8-10 m; Fig. B-5).

Figures B-3 to B-5 do not indicate lateral variations in velocity (i.e., the generally slower velocities of releases upstream of turbines 2 and 10 are not treated separately from releases upstream of the discharging turbine(s)). However, the depth-averaged data indicate that at 3,000 cfs, most water is withdrawn from the bottom of the reservoir (at the depth of the intake), while at the higher discharge rates, withdrawal from shallower reservoir layers above the intake depth also occurs.

The velocity data were averaged over layers appropriate for providing a water flux distribution compatible with the reservoir ecosystem model being developed. Accordingly, the 24 m depth water column at the turbines was divided into 3 layers: 0-6 m, 6-15 m, and 15-24 m. The raw dye velocity data were averaged for each test discharge and layer (Table B-2). Figs. B-6 to B-8 present mean velocities, ± 1 Standard Error interval, for the three layers at each test discharge. This layer averaging shows the same general pattern exhibited by the depth averages (Figs. B-3 to B-5) -- a maximum velocity at the bottom at 3,000 cfs, and more uniform velocity distribution at other discharges.

These layer-average velocities can be used to estimate the fraction of water withdrawn from each layer by each of the three discharges in the same manner as was done for the current meter data (see equation 3 in main report).

The percentage of water coming from each layer (P_i) under any given discharge rate is given by the formula:

$$P_i = \frac{V_i \times D_i}{\sum_{i=1}^{3} V_i * D_i} \qquad (A.3)$$

Table B-1a. Summary of individual dye releases; test discharge = 3000 cfs

OBS	DATE OF RELEASE	TIME OF RELEASE	LATERAL LOCATION OF RELEASE (TURBINE)	PERPENDICULAR DISTANCE FROM DAM (M)	DEPTH OF RELEASE (F)	STRAIGHT-LINE DISTANCE FROM RELEASE (F)	PEAK DYE CONCENTRATION (PPB)	STRAIGHT-LINE VELOCITY (M/SEC)
1	10AUG81	6:27:00	5	50	5.0	50	1.4	0.014
2	12AUG81	7:57:00	5	78	9.5	78	1.1	0.045
3	10AUG81	7:45:00	5	50	10.0	50	4.8	.
4	11AUG81	8:15:00	5	120	10.0	120	.	.
5	10AUG81	5:48:00	5	15	15.0	15	3.1	0.016
6	12AUG81	6:46:00	5	75	16.0	75	3.5	0.039
7	11AUG81	6:20:00	5	70	18.0	70	14.5	0.073
8	11AUG81	7:18:03	5	70	18.0	70	8.8	0.055
9	12AUG81	5:50:00	5	50	18.0	50	0.5	0.019
10	10AUG81	6:40:00	5	7	20.0	7	.	0.058
11	10AUG81	7:07:00	5	50	20.0	50	11.9	0.070
12	12AUG81	5:41:00	5	84	21.5	84	2.6	0.040

Table B-1b. Summary of individual dye releases; test discharge = 5000 cfs.

OPS	DATE OF RELEASE	TIME OF RELEASE	LATERAL LOCATION OF RELEASE (TENTHS)	PERPENDICULAR DISTANCE FROM DAM (M)	DEPTH OF RELEASE (M)	STRAIGHT-LINE DISTANCE FROM RELEASE (M)	PEAK DYE CONCENTRATION (PPB)	STRAIGHT-LINE VELOCITY (M/SEC)
13	31AUG81	9:28:00	5	70	2	70	*	0.050
14	01SEP81	9:26:00	5	70	2	70	*	0.040
15	31AUG81	11:25:00	10	70	2	140	*	*
16	01SEP81	11:04:00	2	70	8	101	*	0.052
17	31AUG81	9:22:00	5	70	8	70	1.8	0.031
18	01SEP81	9:56:00	5	70	8	70	*	0.028
19	31AUG81	11:21:00	10	70	8	140	2.4	0.053
20	01SEP81	11:00:00	2	70	12	101	2.1	0.043
21	31AUG81	8:35:00	5	70	12	70	4.0	0.058
22	01SEP81	9:23:00	5	70	12	70	1.0	0.037
23	01SEP81	11:40:00	10	70	12	140	*	0.042
24	01SEP81	8:40:00	5	70	15	70	*	0.029
25	01SEP81	10:15:00	2	70	18	101	*	0.036
26	31AUG81	8:05:00	5	70	18	70	5.8	0.055
27	01SEP81	8:45:00	5	70	18	70	*	0.027
28	31AUG81	10:47:00	10	70	18	140	3.8	0.045
29	01SEP81	10:12:00	2	70	23	101	*	0.048
30	31AUG81	10:16:00	5	70	23	70	4.9	0.070
31	01SEP81	8:08:00	5	70	23	70	3.0	0.043
32	31AUG81	11:58:00	10	70	23	140	*	*
33	01SEP81	11:43:00	10	70	23	140	4.4	0.048

Table B-1c. Summary of individual dye releases; test discharge = 8000 cfs.

DYE	DATE OF RELEASE	TIME OF RELEASE	LATERAL LOCATION OF RELEASE (TERMINE)	PERPENDICULAR DISTANCE FROM DAM (M)	DEPTH OF RELEASE (F)	STRAIGHT-LINE DISTANCE FROM RELEASE (F)	PEAK DYE CONCENTRATION (PPB)	STRAIGHT-LINE VELOCITY (M/SEC)
34	25AUG81	11:15:00	2	90	2	116	*	*
35	24AUG81	11:04:00	5	55	2	56	1.4	0.046
36	25AUG81	10:13:00	10	75	2	142	*	0.047
37	24AUG81	10:45:00	5	60	8	61	7.0	0.085
38	25AUG81	8:20:00	5	60	4	60	4.6	0.048
39	24AUG81	10:26:00	5	70	12	71	4.2	0.075
40	25AUG81	7:41:00	5	70	12	71	1.7	0.041
41	24AUG81	11:31:00	10	72	12	141	1.9	0.067
42	25AUG81	11:06:00	2	90	18	116	2.1	0.046
43	24AUG81	7:18:00	5	110	18	110	0.2	0.063
44	24AUG81	9:59:00	5	70	18	71	2.5	0.069
45	25AUG81	7:09:00	5	70	18	71	8.8	0.059
46	25AUG81	9:59:00	10	75	18	142	1.9	0.035
47	25AUG81	9:05:00	5	70	22	71	2.1	0.057
48	24AUG81	8:15:00	5	110	23	110		0.041

Table B-2. Dye velocities averaged by test discharge and reservoir layer. Depth = average of all depths in layer; SE = standard error of estimate; Number = number of observations; Lower = average velocity -SE; Upper = average velocity +SE.

OBS	TEST DISCHARGE (CFS)	LAYER	LATERAL LOCATION OF RELEASE (TURBINE)	DATE OF RELEASE	TIME OF RELEASE	DEPTH-AVERAGED DYE VELOCITY (M/SEC)	$\overline{\text{DEPTH}}$	SE
1	3	BOTT	5	12AUG81	6:46:00	0.051	18.7	0.0071
2	3	MID	5	12AUG81	7:57:00	0.030	11.1	0.0141
3	3	SURF	5	12AUG81	8:27:00	0.014	5.0	.
4	5	BOTT	2	01SEP81	10:15:00	0.046	20.7	0.0044
5	5	MID	2	01SEP81	11:04:00	0.042	10.5	0.0036
6	5	SURF	5	31AUG81	9:28:00	0.045	2.0	0.0052
7	8	BOTT	2	25AUG81	11:06:00	0.051	19.2	0.0049
8	8	MID	5	24AUG81	10:45:00	0.064	10.4	0.0085
9	8	SURF	2	25AUG81	11:15:00	0.047	2.0	0.0065

OBS	NUPPER	LOWER	UPPER	DISCHARGE (M3/SEC)
1	7	0.043	0.058	84.9
2	2	0.016	0.045	84.9
3	1	.	.	84.9
4	8	0.042	0.051	141.5
5	9	0.038	0.045	141.5
6	2	0.040	0.050	141.5
7	7	0.046	0.056	226.5
8	5	0.056	0.077	226.5
9	2	0.046	0.047	226.5

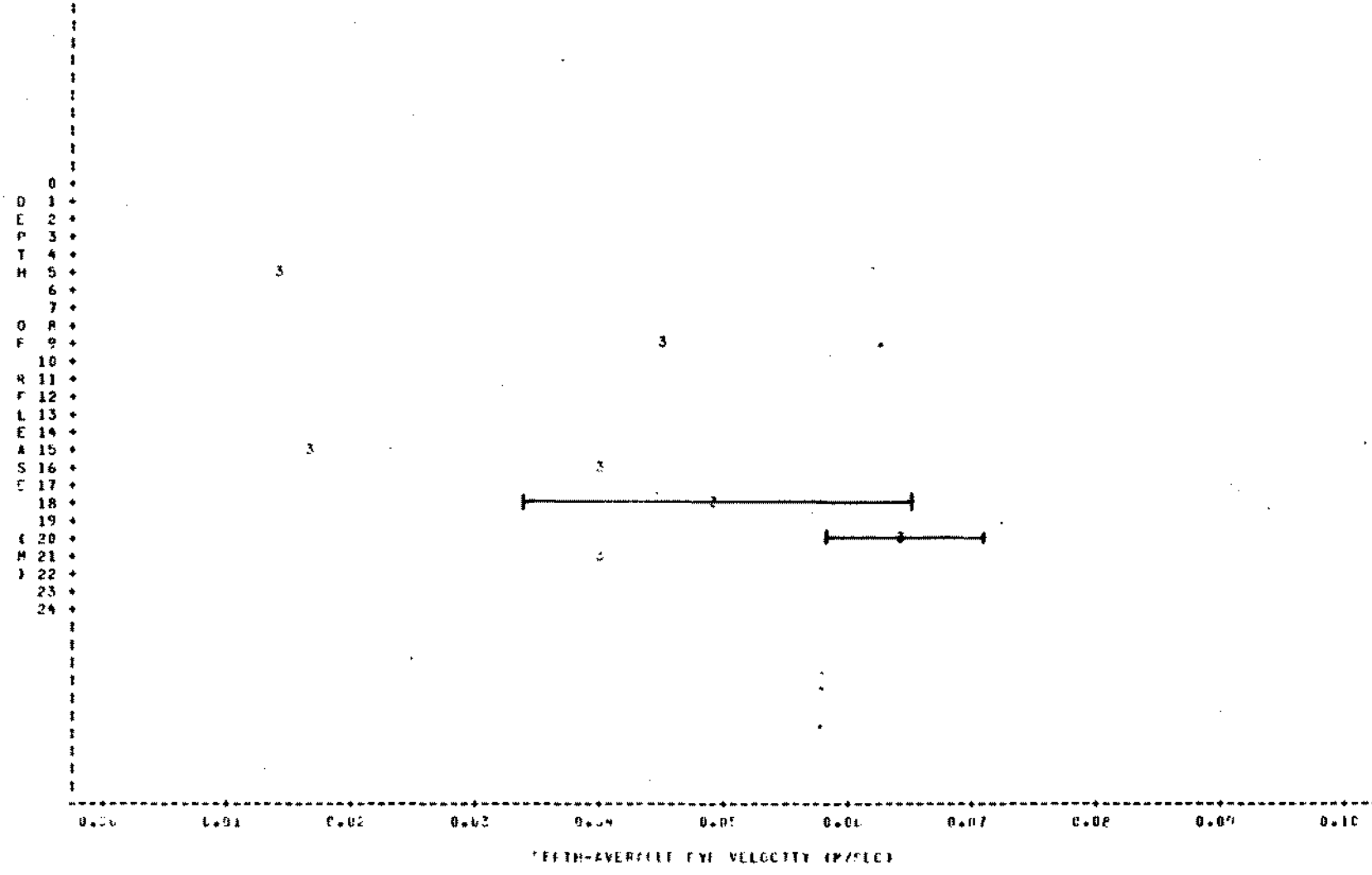

Figure B-3. Dye velocity averaged by depth (with ± 1 SE error bar where multiple releases were made) = 3000 cfs.

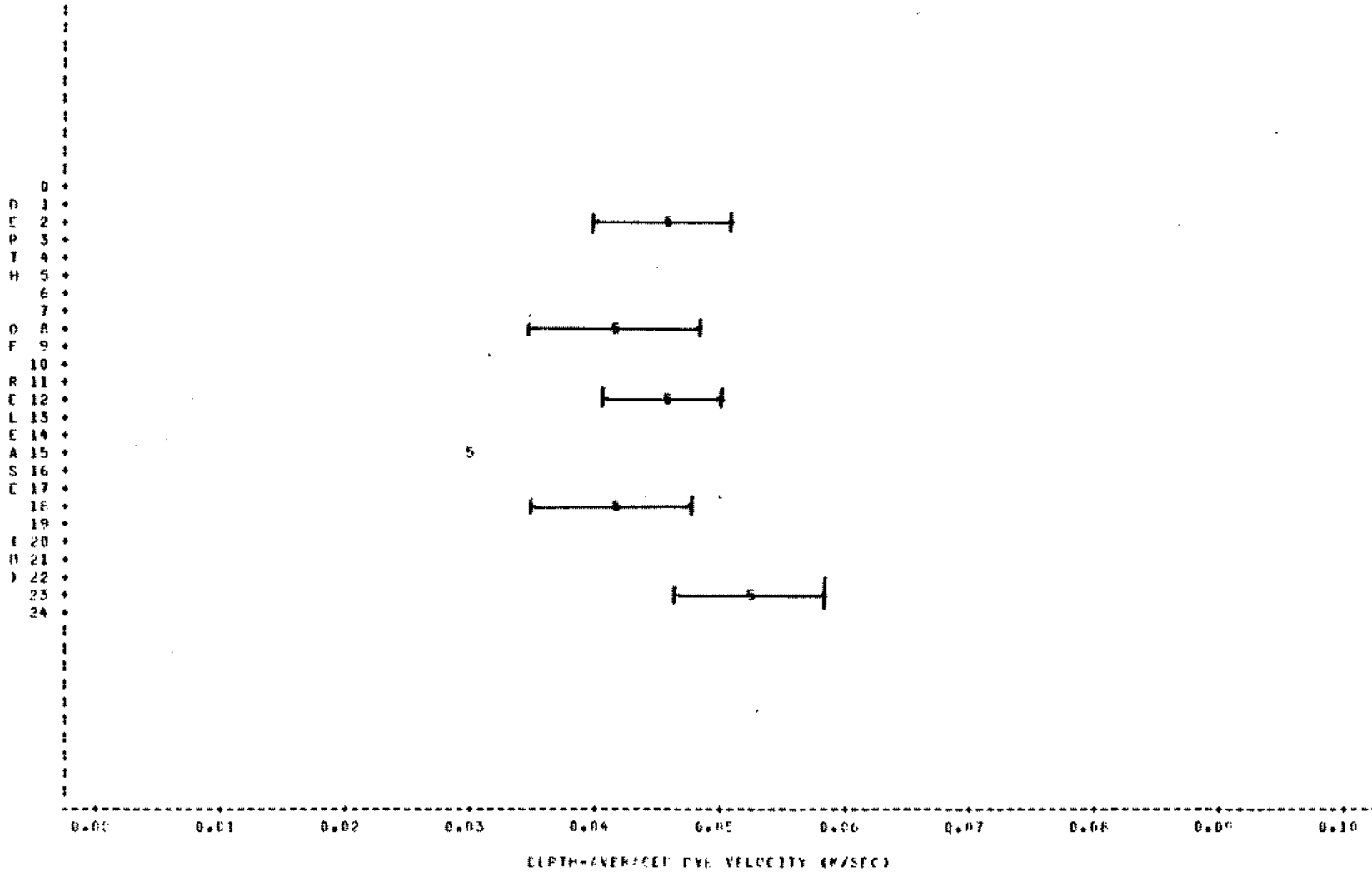

Figure B-4. Dye velocity averaged by depth (with + 1 SE error bar where multiple releases were made) = 5000 cfs.

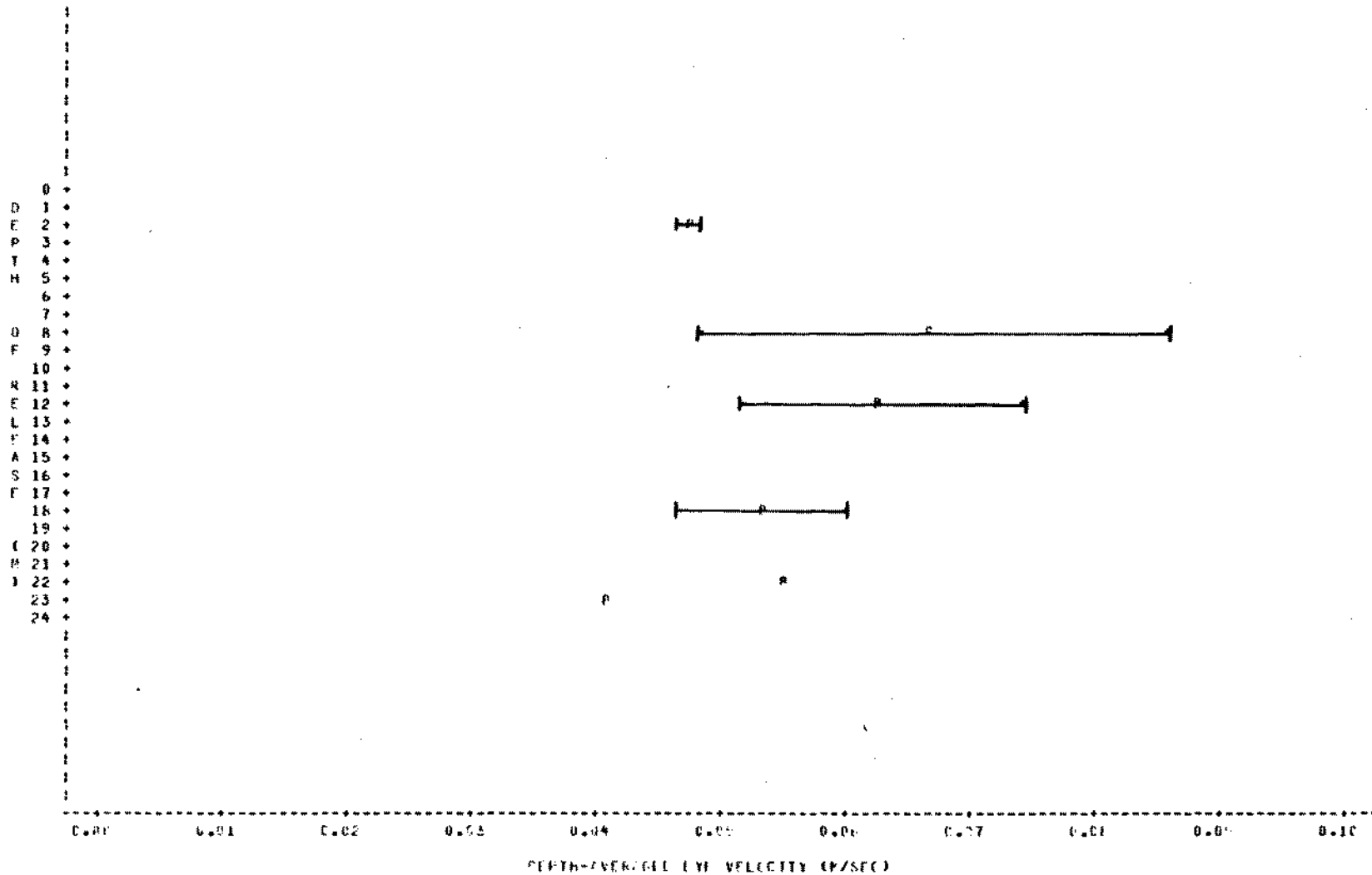

Figure B-5. Dye velocity averaged by depth (with ± 1 SE error bar where multiple releases were made) = 8000 cfs.

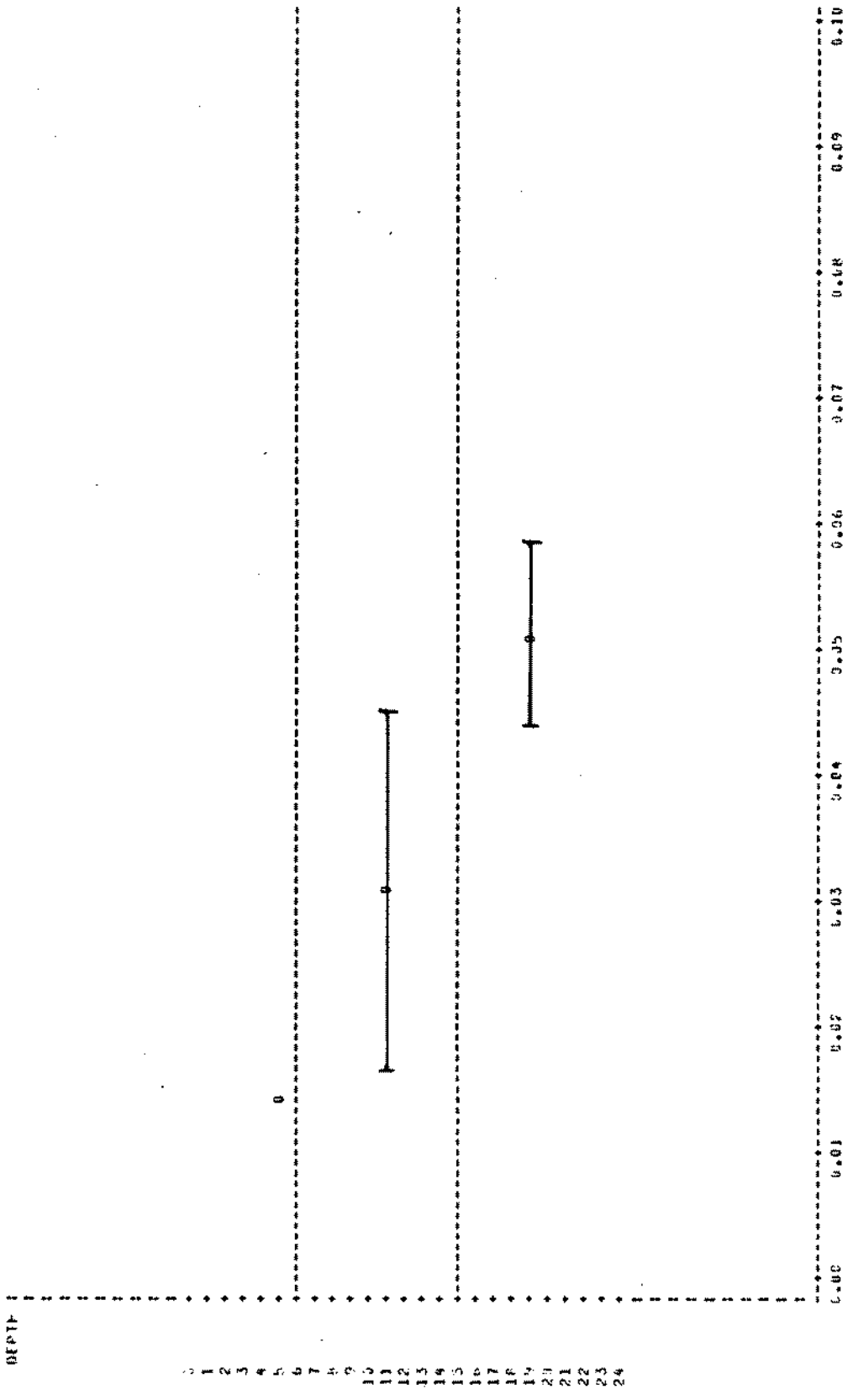

Figure B-6. Dye velocity averaged by layer (with ± 1 SE error bar for multiple observations); test discharge = 3000 cfs.

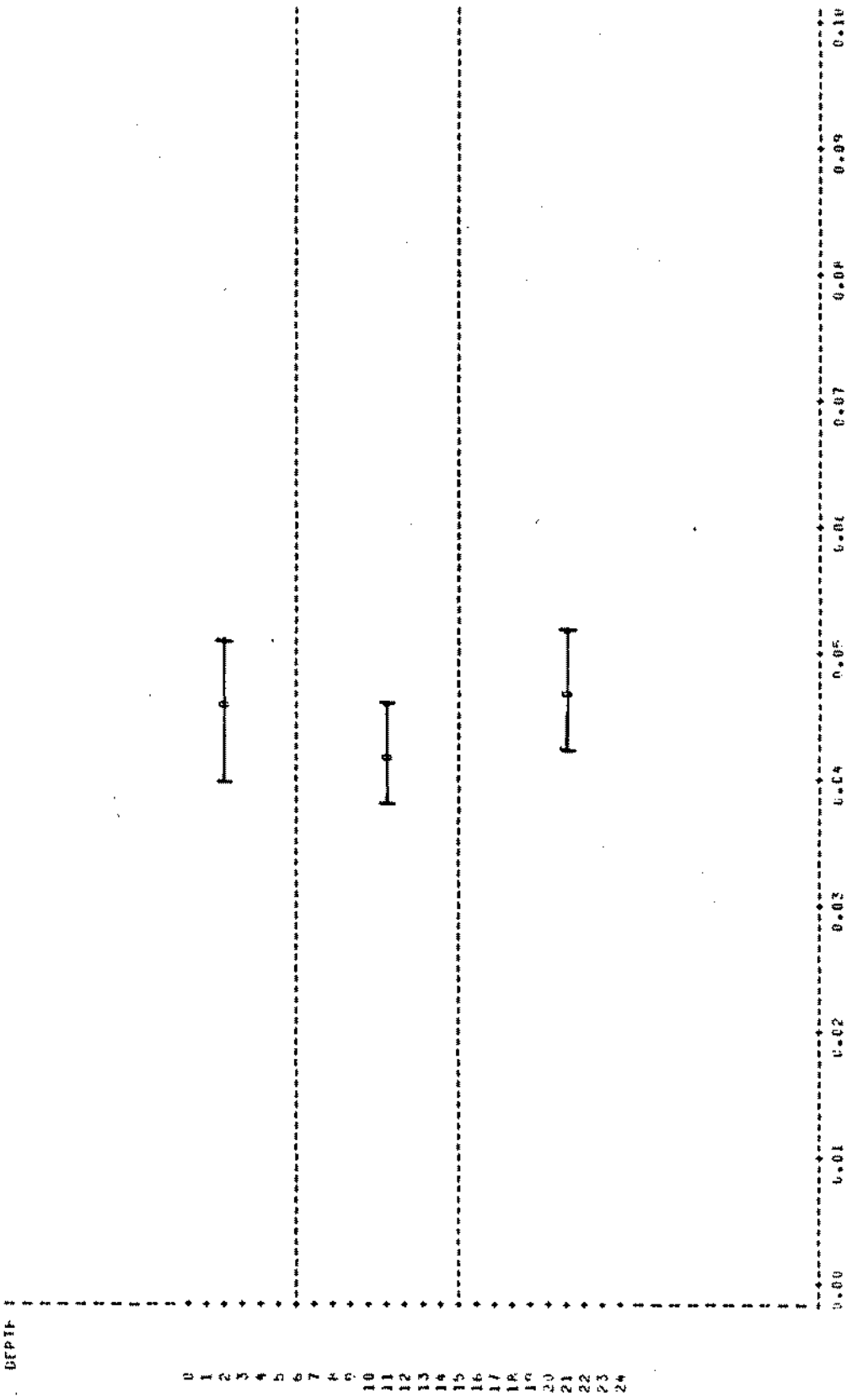

Figure B-7. Dye velocity averaged by layer (with ± 1 SE error bar for multiple observations). test discharge = 5000 cfs.

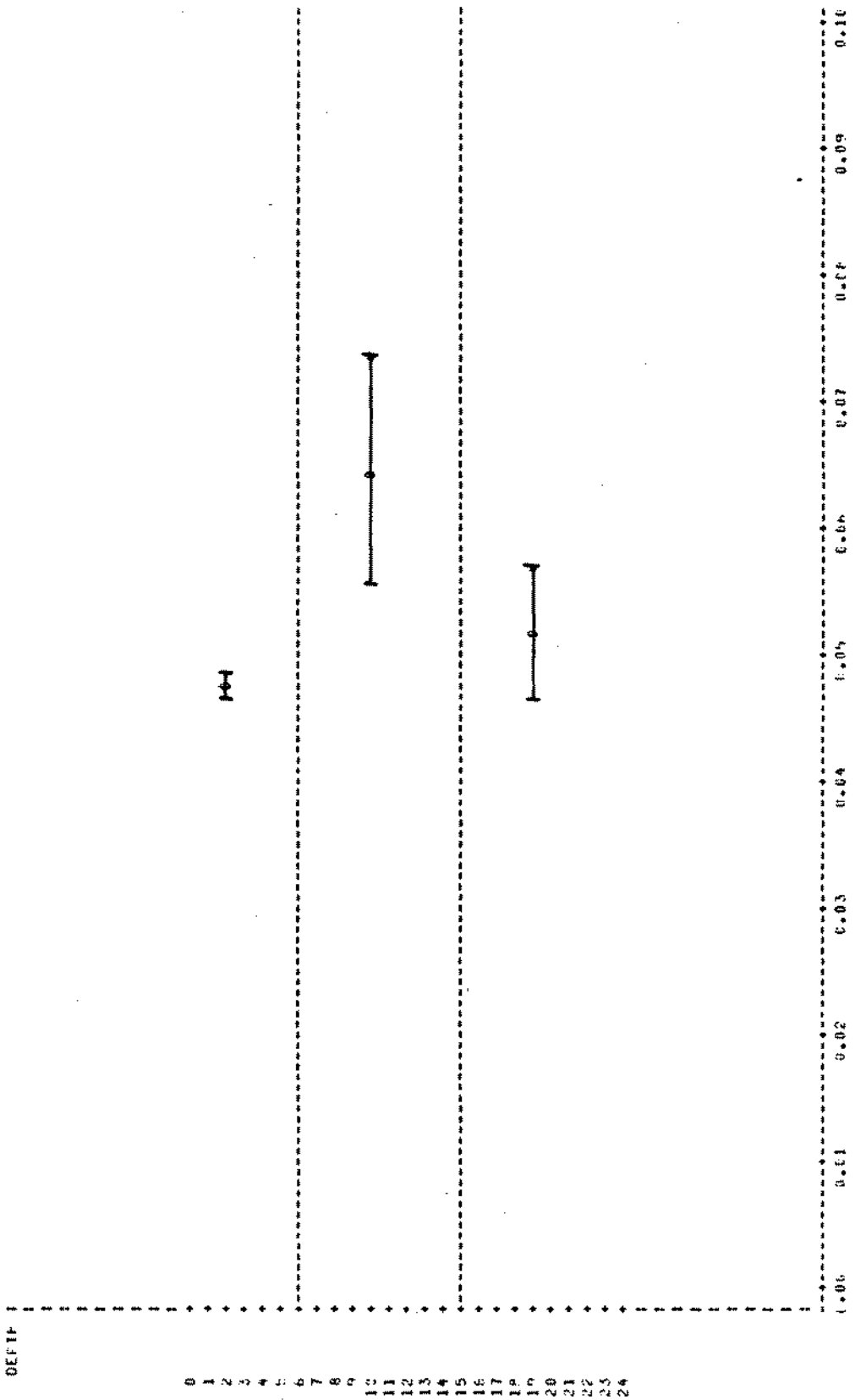

Figure B-8. Dye velocity averaged by layer (with $\pm$ 1 SE error bar for multiple observations); test discharge = 8000 cfs.

where:

P_i = percent of the flow withdrawn from layer i
V_i = average velocity in layer i (m/s)
D_i = thickness of layer i (m)

The quantities $V_i \times D_i$, and the percentages for each layer are presented in Table B-3. Equation A.3, considering that

$$\sum_{i=1}^{3} V_i * D_i = Q,$$

was also solved for W, the hypothetical width over which laterally uniform flux must act to equal the discharge, Q.

Uncertainties in the average dye velocites would be expected to propagate through the calculations to the individual estimates of fractional withdrawal, P_i. However, these calculations are constrained by the interdependence of the relative withdrawal from each layer, as was the case with the estimates made from current meter data.

Table B-3. Fractional withdrawal from each of three layers calculated from dye data, and calculated from current meter data, using Eq. A.3. Also, calculated width of withdrawal (W) in meters.

Test Discharge (cfs)	Fractional Withdrawal from Surface (dye)	Fractional Withdrawal from Surface (current meter)	Fractional Withdrawal from Middle (dye)	Fractional Withdrawal from Middle (current meter)	Fractional Withdrawal from Bottom (dye)	Fractional Withdrawal from Bottom (current data)	W
3000	0.105	0.146	0.338	0.314	0.557	0.540	103.1
5000	0.254	0.177	0.352	0.270	0.394	0.496	131.0
8000	0.213	0.208	0.436	0.337	0.350	0.454	170.3

B.IV. COMPARISON WITH WITHDRAWAL ESTIMATES FROM CURRENT-METER DATA

Layer-averaged withdrawal from current-meter data at 3,000, 5,000, and 8,000 cfs are presented in Table B-3 together with the dye release values.

Although current-meter velocities are generally slower than dye velocities, the relative withdrawal pattern, based on laterally averaging current-meter velocities in each of three layers to compute relative water transport (Eq. A.3), closely corresponds to that determined from the dye data, thus supporting the validity of the general withdrawal model developed. More quantitative comparisons of the two data sets cannot be done because of the small number of dye velocity values (1-9 observations for each of the layer-discharge combinations).

The differences between velocities calculated from current-meter and dye release data can be explained by the fundamental differences between the two methods of measuring velocity. The current meters measure velocities at fixed points in space, while the dye masses follow particles of moving water. Near the dam, water accelerates and converges as it travels toward the turbine intakes. Velocity based on time and distance traveled by a dye mass is actually an average over its trajectory, not the velocity at any one point during transit. A current-meter measurement at the dye release point will thus measure the slowest part of the velocity field experienced by the dye. In Conowingo Reservoir, dye was generally released much closer to the intakes than the locations of the current-meter arrays, which would cause the average dye velocities to be still larger than those measured by current meters.

APPENDIX C: DETAILED CALCULATION OF DISCHARGES UNDER THREE PROPOSED SCHEDULES FOR MINIMUM AND AVERAGE NATURAL RIVER FLOWS IN JULY

C.I. INTRODUCTION

In order to evaluate the effects of minimum discharge schedules (Table I-1) using the linked models, it was first necessary to synthesize, or select from actual operating data, the daily and weekly discharge schedules utilized by the withdrawal model. The model of river hydrodynamics and DO (Dwyer and Turner, 1982) had previously simulated a number of three-day intervals, using actual peaking discharge data as an input at the upstream boundary. To maintain consistency with the river simulations, some of the same three-day segments of discharge data were used as the basis for developing likely operating schedules under the minimum discharge requirements.

This evaluation was intended to test the effectiveness of the minimum discharge requirements under two general river flow conditions:

- Average flows for the month of July (~ 16,000 cfs), and
- The lowest average flow on record for the month of July (~ 4,000 cfs).

C.II. SCENARIOS FOR AVERAGE JULY FLOW CONDITIONS

Two 3-day intervals were selected from the actual discharge record for July 1981, used by Dwyer and Turner (1982):

- A weekday period (Wednesday - Friday) of peaking generation and
- A weekend period (Saturday - Monday) characterized by reduced generation.

Both segments appear to adhere to PECO's proposed minimum discharge schedule (Table I-1). To produce a complete weekly cycle, the missing day (Tuesday) was taken to be the same as Wednesday. The complete Tuesday through Monday week of normal generation was shown in Figure IV-1 of the main report.

SRBC PROPOSAL

During the weekday period the SRBC proposal would require that all shutdown flows be brought up to 5,000 cfs. To simplify the calculations, the scenarios tested in these simulations were based on adding 5,000 cfs to the shutdown flows, instead of bringing the total discharge up to 5,000 cfs. The difference in flows between the SRBC proposal and the tested scenario was judged to be negligible. To compensate for this non-peak water consumption, each peaking discharge following a shutdown period was reduced uniformly to the point where the amount of water required to provide the minimum flow for the shutdown period was reached. The required reductions ranged from 3,150 to 3,600 cfs for each of the three periods where peak generation exceeded 20,000 cfs. Peaking discharges on the days of the weekend had to be greatly reduced to provide the minimum flow. One weekend peak was eliminated entirely, and the Monday peak was reduced by 6,900 cfs. The complete weekly discharge schedule under the SRBC proposal is shown in Figure IV-1 of the main report.

FERC STAFF PROPOSAL

On weekdays, the FERC propoal requires that all shutdown flows be brought up to 3,000 cfs. To simplify the calculations, the scenarios tested in these simulations were based on adding 3,000 cfs to the shutdown flows, rather than on bringing the total discharge up to 3,000 cfs. Again, the difference between the two was judged to be negligible. Compensating reductions of peaks on the three weekdays ranged from 1,765 to 2,175 cfs for discharges greater than 20,000 cfs. During weekend days, discharge increases (above shutdown) of 3,000 cfs required elimination of the single peak, reduction of a period of 10,000 cfs discharge to 3,000 cfs, and reduction of the Monday peak discharge (above 20,000 cfs) by 3,750 cfs. The complete 7-day cycle is shown in Figure IV-1 of the main report.

GENERATION SCHEDULE WITH A MINIMUM DISCHARGE OF 11,000 CFS (~ TWO SMALL TURBINES)

To meet this discharge requirement, peaks greater than 37,000 cfs were reduced by approximately 16,000 cfs, and peaks between 11,000 and 37,000 cfs were reduced to 11,000 to compensate for the minimum discharge. On the weekend, the 11,000 cfs requirement completely eliminated the peaks, and reduced the Monday peak somewhat. See Figure IV-2 of the main report.

RUN-OF-RIVER GENERATION

This is a continuous discharge at 16,000 cfs, the equivalent of the capacity of three small turbines. See Figure IV-2 of the main report.

C.III. SCENARIOS FOR LOWEST AVERAGE JULY FLOWS

Presuming a three-day period under 4,000 cfs average river flow, the total amount of water available is 72 hr x 4,000 cfs = 288,000 cfs-hr (a unit reflecting the volume of a 1 cfs discharge maintained for 1 hour).

PECO PROPOSAL

PECO's proposed schedule would require at least six 4-hr periods of generation at 5,000 cfs: 5,000 cfs x 4 hr x 6 periods = 120,000 cfs-hr used for minimum flow. The remainder, 168,000 cfs-hr, is available for peaking. If all of this is used as a peaking increment to the minimum flow for four hours on Monday afternoon (when power is more valuable than on weekends), then the peak discharge is: 168,000 cfs-hr/4 hr = 42,000 cfs + 5,000 cfs minimum = 47,000 cfs.

Peaking generation is of most value on weekday afternoons. This 47,000 cfs peak can be assumed to occur near the interval of 1400-1800 on Monday. The 4-hr 5,000 cfs releases would thus occur at 0200-0600 (flushing the river at the time of the DO minimum) and at 1400-1800 on other weekdays, assuming 8-hr shutdown periods between releases.

On a weekday schedule, the 168,000 cfs-hr is divided among three afternoon peaking periods, each 4 hours long:

$$168{,}000/(3 \times 4\ \text{hr}) = 14{,}000\ \text{cfs}$$
$$+ 5{,}000\ \text{cfs minimum}$$
$$= 19{,}000\ \text{cfs}$$

with a 4 hour-5,000 cfs discharge in the morning of each day.

The complete 7-day cycle is shown in Figure IV-5 of the main report.